



# Ice Complex permafrost of MIS5 age in the Dmitry Laptev Strait coastal region (East Siberian Arctic)



Sebastian Wetterich <sup>a,\*</sup>, Vladimir Tumskoy <sup>b,c</sup>, Natalia Rudaya <sup>d,e,f,g</sup>,  
Vladislav Kuznetsov <sup>h</sup>, Fedor Maksimov <sup>h</sup>, Thomas Opel <sup>a</sup>, Hanno Meyer <sup>a</sup>,  
Andrei A. Andreev <sup>g,i</sup>, Lutz Schirrmeister <sup>a</sup>

<sup>a</sup> Alfred Wegener Institute, Helmholtz Center for Polar and Marine Research, Department of Periglacial Research, Potsdam, Germany

<sup>b</sup> Lomonosov Moscow State University, Faculty of Geology, Russia

<sup>c</sup> National Research Tomsk Polytechnic University, Russia

<sup>d</sup> Institute of Archaeology and Ethnography, SB RAS, Novosibirsk, Russia

<sup>e</sup> Novosibirsk State University, Russia

<sup>f</sup> Altai State University, Barnaul, Russia

<sup>g</sup> Kazan Federal University, Institute of Geology and Petroleum Technologies, Russia

<sup>h</sup> St. Petersburg State University, Institute of Earth Sciences, Köppen Laboratory, Russia

<sup>i</sup> University of Cologne, Institute of Geology and Mineralogy, Germany

## ARTICLE INFO

### Article history:

Received 26 March 2015

Received in revised form

30 October 2015

Accepted 20 November 2015

Available online 18 December 2015

### Keywords:

Cryostratigraphy

Palaeoenvironments

<sup>230</sup>Th/U dating

Permafrost

Bol'shoy Lyakhovsky Island

Oyogos Yar

Beringia

Marine Isotope Stage 5

## ABSTRACT

Ice Complex deposits (locally known as the Buchchagy Ice Complex) are exposed at both coasts of the East Siberian Dmitry Laptev Strait and preserved below the Yedoma Ice Complex that formed during MIS3 and MIS2 (Marine Isotope Stage) and lateglacial-Holocene thermokarst deposits (MIS1). Radio-isotope disequilibria ( $^{230}\text{Th}/\text{U}$ ) of peaty horizons date the Buchchagy Ice Complex deposition to  $126 + 16/-13$  kyr and  $117 + 19/-14$  kyr until  $98 \pm 5$  kyr and  $89 \pm 5$  kyr. The deposit is characterised by poorly-sorted medium-to-coarse silts with cryogenic structures of horizontal ice bands, lens-like, and lens-like reticulated segregation ice. Two peaty horizons within the Buchchagy Ice Complex and syngenetic ice wedges (2–4 m wide, up to 10 m high) are striking. The isotopic composition ( $\delta^{18}\text{O}$ ,  $\delta\text{D}$ ) of Buchchagy ice-wedge ice indicates winter conditions colder than during the MIS3 interstadial and warmer than during MIS2 stadial, and similar atmospheric winter moisture sources as during the MIS2 stadial. Buchchagy Ice Complex pollen spectra reveal tundra-steppe vegetation and harsher summer conditions than during the MIS3 interstadial and rather similar vegetation as during the MIS2 stadial. Short-term climatic variability during MIS5 is reflected in the record. Even though the regional chronostratigraphic relationship of the Buchchagy Ice Complex to the Last Interglacial remains unclear because numerical dating is widely lacking, the present study indicates permafrost (Ice Complex) formation during MIS5 *sensu lato*, and its preservation afterwards. Palaeoenvironmental insights into past climate and the periglacial landscape dynamics of arctic lowlands in eastern Siberia are deduced from the record.

© 2015 Elsevier Ltd. All rights reserved.

## 1. Introduction

Late Pleistocene ice-rich permafrost deposits with syngenetic ice-wedges (Ice Complex, IC) are widespread in the East Siberian Arctic (Schirrmeister et al., 2011a) and have analogues in formations found in north-western Siberia (e.g. Streletskaya et al., 2013), Alaska (e.g. Kanevskiy et al., 2011), and Canada (e.g. Froese et al.,

2009). An Ice Complex (ледовый комплекс [ledovyi kompleks] in Russian) as defined by Solov'ev (1959) includes syngenetic ice wedges (IW, grown synchronously with sediment deposition), fine-grained ice-rich sediments, and a considerable amount of organic material (Strauss et al., 2012, 2013). Such deposits preserve late Quaternary records of the Beringian tundra-steppe ecosystems that maintained the Mammoth fauna. The most prominent IC type is termed Yedoma. It formed during MIS3 and MIS2 between about >55 and 13 kyr BP in eastern Siberia (Schirrmeister et al., 2011a). Yedoma ICes have been extensively studied for their origin (for

\* Corresponding author.

E-mail address: [sebastian.wetterich@awi.de](mailto:sebastian.wetterich@awi.de) (S. Wetterich).

overview see Schirrmeister et al., 2013), distribution (Grosse et al., 2013), cryolithological (e.g. Schirrmeister et al., 2011a) and palaeoenvironmental inventories (e.g. Wetterich et al., 2008), biogeochemical properties (Schirrmeister et al., 2011b; Strauss et al., 2014), and fate under arctic warming (Zimov et al., 2006; Schneider von Deimling et al., 2014). An IC pre-dating the Yedoma type has rarely been found and investigated, although such research is relevant for understanding how glacial–interglacial dynamics shape the geoecosystem response to climate variations. The oldest known IC is named the Yukagir IC; it was studied at the mainland coast of Cape Svyatoi Nos (Nikolsky et al., 1999; Nikolsky and Basilyan, 2004) and at the southern coast of Bol'shoy Lyakhovsky Island (New Siberian Archipelago; Fig. 1) (Arkhangelov et al., 1996; Andreev et al., 2004). Here, coastal exposures are considered to be one of the longest-spanning late Quaternary permafrost archives in East Siberia (Andreev et al., 2011). Mid-Pleistocene (MIS7a) peat of the Yukagir IC was dated by  $^{230}\text{Th}/\text{U}$  (thorium-230/uranium-234) radioisotope disequilibrium to  $200.9 \pm 3.4$  kyr (Schirrmeister et al., 2002), and studied for its palaeoecology (unit I, late Saalian IC deposits in Andreev et al., 2004). Later investigations on the stratigraphy of Bol'shoy Lyakhovsky Island found another IC older than the Yedoma type that

was termed the Buchchagy IC (named after the Buchchagy River; Tumskoy and Basilyan, 2006, 2009; Tumskoy, 2012).

The major aims of the present study are (1) to provide geochronological evidence for the age of the Buchchagy IC by  $^{230}\text{Th}/\text{U}$  radioisotope disequilibrium dating, (2) to characterise the cryolithological properties of the Buchchagy IC and its palaeoenvironmental indication, (3) to evaluate its stratigraphic position along both coasts of the Dmitry Laptev Strait in regional context, and (4) to deduce the formation and preservation conditions of the Buchchagy IC in context of late Quaternary glacial–interglacial dynamics in western Beringia.

## 2. Study region

The Dmitry Laptev Strait connects the Laptev and the East Siberian seas south of the New Siberian Archipelago (Fig. 1). The region is in the continuous permafrost zone with permafrost depths of 500–600 m and permafrost temperatures of  $-15$  to  $-11$  °C (Zaitsev et al., 1989). The coastal interfaces between the Dmitry Laptev Strait and both shores are characterised by rapid coastal retreat. Pizhankova and Dobrynina (2010) estimated erosion rates of 3.6 m per year for late Pleistocene Yedoma IC sections and of

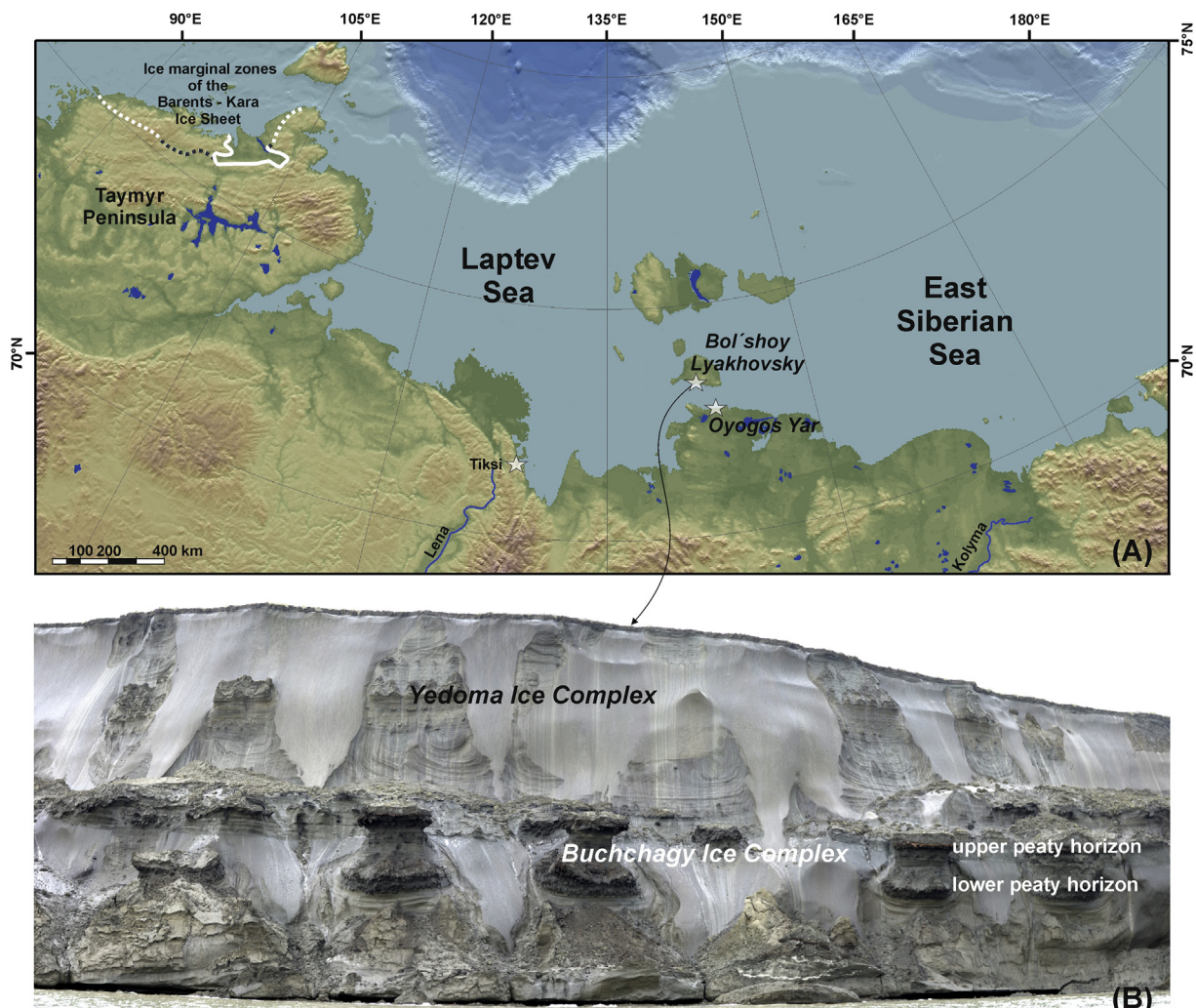


**Fig. 1.** Study region at the Dmitry Laptev Strait including (A) the southern coast of Bol'shoy Lyakhovsky Island and the Oyogos Yar mainland coast, and (B) an image of coastal outcrops on Bol'shoy Lyakhovsky Island exposing the Buchchagy Ice Complex below the Yedoma Ice Complex. The ice marginal zones of the Barents-Kara Ice Sheet on northern Taymyr Peninsula is indicated by a white dotted line for MIS5d-5b, by a grey dotted line for MIS4 and by a white line for MIS2 redrawn from Möller et al. (2015).

3.4 m per year for Holocene thermokarst sections at the southern coast of Bol'shoy Lyakhovsky Island. Similar estimates, although obtained using a different approach, were given by Günther et al. (2013) for the Oyogos Yar mainland coast, with coastal retreat rates of 2.85 m per year for Yedoma IC sections and 3.38 m per year for thermokarst sections. Rapidly retreating coastlines provide access to the geological inventory of late Quaternary permafrost and uncover frozen sediments, ground ice, and fossil remains dating from the mid-Pleistocene (MIS7a) onward at the southern coast of Bol'shoy Lyakhovsky Island (Schirmeister et al., 2002; Andreev et al., 2004). The opposite mainland coast, Oyogos Yar, offers a similar stratigraphic composition at least from the Last Interglacial onward (Tumskoy, 2012).

Numerous studies of different stratigraphic horizons exposed at both coasts of the Dmitry Laptev Strait have been undertaken so far, unfolding the natural history of north-eastern Siberia (e.g. Romanovskii, 1958; Ivanov, 1972; Konishchev and Kolesnikov, 1981; Kunitsky, 1998; Meyer et al., 2002; Andreev et al., 2004, 2009; Ilyashuk et al., 2006; Kienast et al., 2011; Opel et al., 2011; Wetterich et al., 2009, 2011, 2014).

The geological inventory of permafrost coasts at the Dmitry Laptev Strait comprises at least three generations of stadial or interstadial IC deposits intersected by deposits of the Last Interglacial and covered by Holocene deposits (Tumskoy, 2012). The preservation of single sections is spatially variable since the impact of warm-stage ground ice melt and subsequent permafrost degradation (i.e. thermokarst) is dictated by different palaeo-relief conditions. As a result the modern landscape morphology is typically characterised by uplands preserving late Pleistocene ice-rich Yedoma IC, lateglacial-Holocene thermo-erosional valleys, and thermokarst basins that formed when older permafrost degraded.

The Buchchagy IC is exposed in places along the southern coast of Bol'shoy Lyakhovsky Island, east of the Zimov'e River mouth, and at the Oyogos mainland coast, west of the Kondrateva River mouth (Fig. 1). The Buchchagy IC is either preserved below the Yedoma IC or below Holocene deposits (Fig. 2) if the Yedoma degraded during the lateglacial-Holocene warming. Ice-poor sandy and silty deposits underlying the Buchchagy IC are termed the Kuchchugui stratum (Ivanov, 1972). However, the stratigraphic position of the Kuchchugui stratum is still in question due to a lack of appropriate chronostratigraphic data (unit IIa, late Saalian [pre-Eemian] floodplain deposits and unit IV, early Weichselian [post-Eemian] floodplain deposits in Andreev et al., 2004).

The Buchchagy IC is considered to be stratigraphically significant on the regional scale because similar structures have been observed along both coasts of the Dmitry Laptev Strait, extending over tens of kilometres (Tumskoy and Dobrynin, 2008).

### 3. Materials and methods

#### 3.1. Fieldwork

The Buchchagy IC exposures were studied and sampled at the southern coast of Bol'shoy Lyakhovsky Island (Fig. 2; 73.28661°N; 141.7052°E), and at the Oyogos Yar mainland (Fig. 3; 72.672°N; 143.63514°E) in summer 2007 during the joint Russian–German 'Lena – New Siberian Islands' expedition (Boike et al. [eds.], 2008).

The cryolithological features of the Buchchagy IC on Bol'shoy Lyakhovsky Island (profile L7-15) were described and sampled using climbing equipment on a steep wall between 3 and 13.5 m above sea level (m a.s.l.). Fourteen frozen sediment samples of profile L7-15 were taken every 0.5–1 m using knife and hammer in one subprofile between two ice wedges; an additional of eight samples of the underlying deposits were taken in a second subprofile (Fig. 2). The syngenetic ice wedge between both subprofiles

was sampled in a horizontal transect of nine samples using ice screws at about 6 m a.s.l. (Fig. 2).

The studied exposure on Oyogos Yar (Oy7-10), which was only accessible between 2 and 6.2 m a.s.l., was cryolithologically described and probed in nine sediment samples (Fig. 3). Ice wedges were not sampled here due to limited outcrop accessibility.

Both exposures include samples from two distinct (lower and upper) peaty horizons that are considered as characteristic for the Buchchagy IC (Tumskoy, 2012).

The gravimetric ice content of the frozen deposits was estimated immediately after thawing by comparing the weight of the frozen sample to the weight of the oven-dried sample, expressed as weight percentage (wt%) (van Everdingen, 1998). Ice oversaturation of the deposits is indicated by values higher than 100 wt%.

#### 3.2. Sediment and ground ice studies

Upon return to the laboratory the sediment samples were freeze-dried, carefully manually homogenised, and split into subsamples for sedimentological, geochemical, and palynological analyses. Grain-size distribution was analysed using a laser-particle analyser (Beckmann Coulter LS 200) and computed with GRADISTAT 4.0 software (Blott and Pye, 2001). A Bartington MS2 instrument (MS2B sensor) was used to measure mass-specific magnetic susceptibility (MS), given in SI units (Le Système International d'Unités,  $10^{-8} \text{ m}^3 \text{ kg}^{-1}$ ). The total organic carbon (TOC) and total nitrogen (TN) contents were measured by a carbon–nitrogen–sulphur (CNS) analyser (Elementar Vario EL III), and the carbon to nitrogen ratio (C/N) was calculated as TOC/TN. Stable carbon isotopes ( $\delta^{13}\text{C}$ ) in TOC were measured with a Finnigan DELTA S mass spectrometer coupled to a FLASH element analyser and a CONFLO III gas mixing system after removal of carbonates with 10% HCl in Ag-cups and combustion to CO<sub>2</sub>. Accuracy of the measurements was determined by parallel analysis of internal and international standard reference material. The analyses were accurate to  $\pm 0.2\text{\textperthousand}$ . The  $\delta^{13}\text{C}$  values are expressed in delta per mil notation ( $\delta, \text{\textperthousand}$ ) relative to the Vienna Pee Dee Belemnite (VPDB) Standard.

Samples from the L7-15 ice wedge (Fig. 2) were analysed for stable water isotope composition ( $\delta^{18}\text{O}, \delta\text{D}$ ). The deuterium (d) excess, defined as  $d = \delta\text{D} - 8 * \delta^{18}\text{O}$ , was calculated according to Dansgaard (1964) and interpreted as an indicator of secondary kinetic fractionation processes during ice formation. Equilibration technique was applied using a mass spectrometer (Finnigan MAT Delta-S) with reproducibility derived from long-term standard measurements of  $1\sigma$  better than  $\pm 0.1\text{\textperthousand}$  for  $\delta^{18}\text{O}$  and  $\pm 0.8\text{\textperthousand}$  for  $\delta\text{D}$  (Meyer et al., 2000). All samples were run at least in duplicate. The values are given as  $\delta, \text{\textperthousand}$  relative to the Vienna Standard Mean Ocean Water (VSMOW) Standard. Supernatant water from 20 sediment samples (14 samples of L7-15 and 6 samples of Oy7-10), i.e. from thawed segregation (texture) ice, was likewise analysed to study past ground freezing conditions.

#### 3.3. Radiocarbon dating

Botanically indeterminable fossil plant fragments from four samples from the lower and upper peaty horizons of both studied profiles were radiocarbon-dated using the accelerator mass spectrometry (AMS) facility of the Poznań Radiocarbon Laboratory (Adam Mickiewicz University, Poznań, Poland). Details on laboratory procedures are given by Goslar et al. (2004), while a broad discussion of radiocarbon dating of syngenetic permafrost is given in Vasil'chuk and Vasil'chuk (2014) and Wetterich et al. (2014).

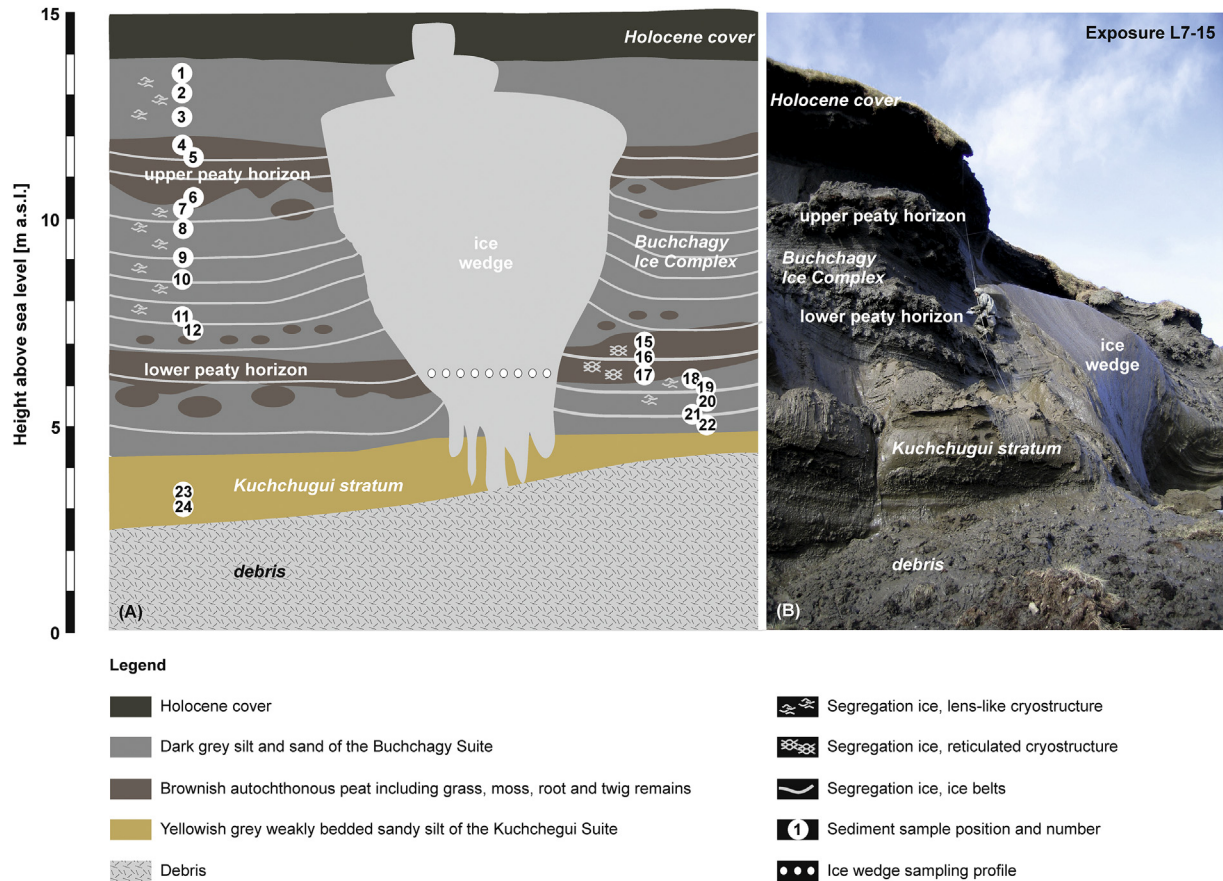


**Fig. 2.** Schematic (A) and photograph (B) of profile L7-15 (Buchchagy Ice Complex, Bol'shoy Lyakhovsky Island) indicating sampling positions (numerals) and main cryolithological features.

### 3.4. $^{230}\text{Th}/\text{U}$ dating

Radiochemical analyses of  $^{230}\text{Th}/\text{U}$  disequilibria in the lower peaty horizon from the L7-15 profile were performed at the Radioisotope Geochronological Laboratory (Köppen-Lab) of the St. Petersburg State University using Alpha Spectrometry. The applied isochronous approach combines analytical data obtained from five subsamples of the dated probe. The isochronous approximation is based on agreement with isochronous-corrected ages obtained for the same coeval samples analysed using two different analytical techniques based on (1) acidic extraction of a sample in leachate alone (L/L model), and on (2) total sample dissolution (TSD model), in order to improve the precision and reliability of the radioisotope dating (Maksimov and Kuznetsov, 2010). Details of laboratory procedures and sample processing are given in Maksimov and Kuznetsov (2010), Maksimov et al. (2011), Kuznetsov and Maksimov (2012) and Börner et al. (2015). Alpha-spectrometric measurements of the U and Th isotopes enabled to determine  $^{238}\text{U}$ ,  $^{234}\text{U}$ ,  $^{232}\text{Th}$ , and  $^{230}\text{Th}$  specific activities and their activity ratios (ARs). The  $^{230}\text{Th}/\text{U}$  age of the peaty layer was calculated with standard deviation error  $\pm 1\sigma$  according to the isochronous approximation (Geyh, 2001; Geyh and Müller, 2005), applying the equation proposed by Kaufman and Broecker (1965).

### 3.5. Palynology

A total of 22 samples from profile L7-15 and nine samples from profile Oy7-10, each consisting of two grams of dry sediment, were prepared for pollen analysis using standard procedures including

treatment with HCl and KOH, sieving ( $250 \mu\text{m}$ ), treatment with HF, acetolysis, and mounting in glycerin (cf. Fægri and Iversen, 1989). Two *Lycopodium* spore tablets were added to each sample in order to calculate total pollen and spore concentrations (cf. Stockmarr, 1971). Pollen and spore residues mounted in glycerin were analysed under a Zeiss AxioImager D2 light microscope at  $400\times$  magnification. Identification of pollen and spores was performed using a reference pollen collection and pollen atlases (Beug, 2004; Kuprianova and Alyoshina, 1972). Non-pollen palynomorphs (NPPs) were identified using descriptions, sketches, and photographs published by Jankovska (1991) and van Geel (2001). Percentages of all taxa were calculated based on setting the total of all pollen and spore taxa equal to 100%. Results of pollen analysis are displayed in the pollen diagrams produced with the Tilia/TiliaGraph software (Grimm, 2004). The visual definition of the pollen zones (PZs) is supported by CONISS software.

## 4. Results

### 4.1. Sediment and ground ice characteristics

The Buchchagy IC sediments are ice-rich poorly-sorted medium-to-coarse silts (mean grain size of  $25\text{--}56 \mu\text{m}$ ; Figs. 4 and 5). The cryogenic structures are horizontal ice bands, lens-like and lens-like-reticulated segregation ice. Syngenetic ice wedges ( $2\text{--}4 \text{ m}$  wide, up to  $10 \text{ m}$  high) with clearly expressed "shoulders" as well as two distinct peaty horizons up to  $1 \text{ m}$  thick within the frozen deposits define the Buchchagy IC (Fig. 2). The vertical distance between both peaty horizons is about  $3 \text{ m}$ . The total thickness

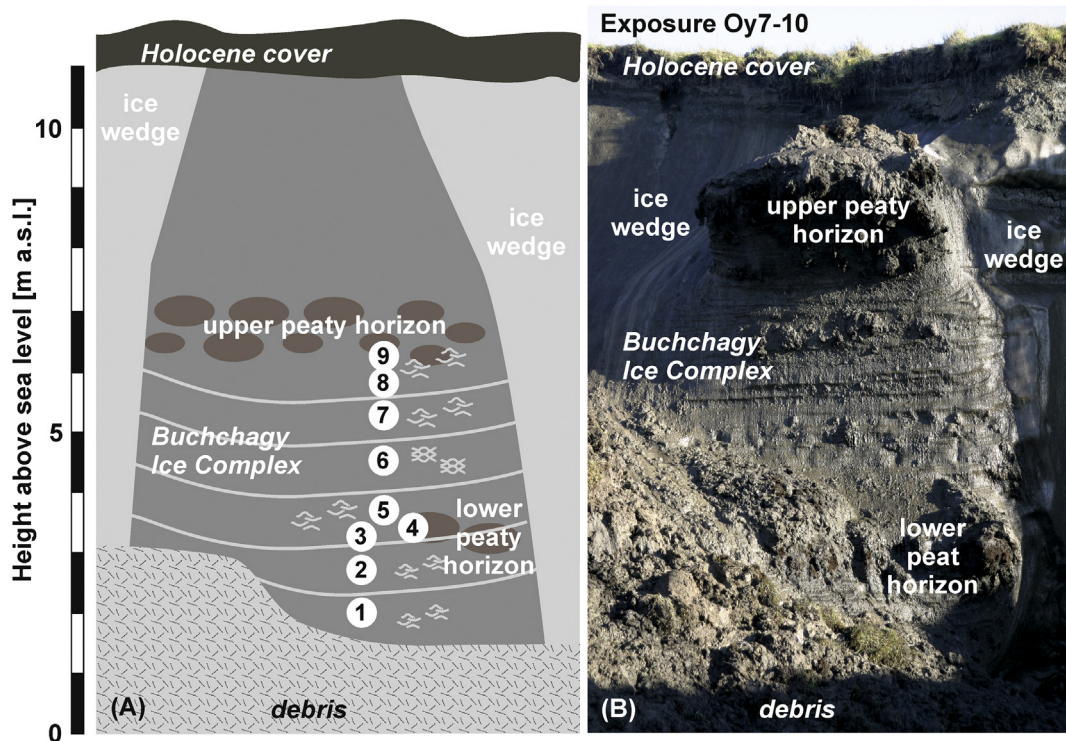


**Fig. 3.** Schematic (A) and photograph (B) of profile Oy7-10 (Buchchagy Ice Complex, Oyogos Yar coast) indicating sampling positions (numerals) and main cryolithological features. The legend is given in Fig. 2.

of the Buchchagy IC reaches 6–8 m. The transformation to deposits of the underlying ice-poor Kuchchugui stratum is mainly detectable by changes in the cryostructure from ice-rich banded and lens-like to massive (meaning no visible ice) and micro-lensed.

The Kuchchugui stratum was sampled in the lower part of the L7-15 profile between 2 m and 3.5 m a.s.l. (Fig. 2). It is composed of light grey to brownish irregular laminated fine-grained sand containing numerous grass roots. Platy organic inclusions (about  $7 \times 2$  cm) were observed to be typical for the Kuchchugui stratum. TOC content reaches 1.4 wt% and TN 0.15 wt% (TOC/TN = 9.6) in the peat inclusions. The  $\delta^{13}\text{C}$  varies between  $-28.3$  and  $-26.1\text{\textperthousand}$ . The cryostructure is massive, but the ice content of 99 wt% is however relatively high (Fig. 4a). The deposits of the Kuchchugui stratum below the lower peaty horizon resemble the units IIa and IV described in Andreev et al. (2004). Upwards the ice content reaches over 100 wt% and exhibits maximum values of about 226 wt% in the lower peaty horizon where 3–4 cm thick ice bands and coarse lens-like-reticulated cryostructures between the ice bands occur. The lower peaty horizon (between about 6 and 7 m a.s.l.) consists of dark-brown large peat inclusions (20–30 cm in diameter) and a greyish silt matrix. Above the lower peaty horizon an ice-rich horizon about 3 m thick (between about 7 and 10 m a.s.l.) consists of greyish silt with 1–3 cm thick ice bands and lens-like cryostructures in between. Single ice veins are 1–1.5 mm thick and occur 5–10 mm apart. The ice content varies between 69 and 106 wt%. Several small peat lenses (less than 10 cm in diameter) are present at about 10 m a.s.l. and mark the transition into the upper peaty horizon (between about 10 and 12 m a.s.l.). The latter consists of numerous dark-brown peat lenses in a matrix of greyish silt with banded cryostructures (1.5–2 cm thick 5–10 cm apart). Brown weakly-bedded silt (between about 12 and 14 m a.s.l.) overlies the upper peaty horizon, and contains rare peat and small wood fragments (2–3 mm in diameter). The cryostructure here exhibits microlenses and the ice content is below 30 wt%. Single ice lenses

are 2 mm thick and 5–15 mm long. The sequence is capped by the loamy deposits of a thermo-erosional valley (between about 14 and 15 m a.s.l.; not sampled).

The granulometrical properties of the Buchchagy IC vary widely below the lower peaty horizon and then change gradually to smaller grain size, while the sand fraction decreases. Poorly-sorted silt comprises the entire profile (Fig. 5a). MS values are higher, >30 SI, in the lower peaty horizon, and lower in the upper peaty horizon. MS values in the uppermost part (above the upper peaty horizon) increase again to >30 SI (Fig. 4a). The overall MS values range between 19 and 37 SI, indicating changing magnetic properties in the Buchchagy IC source material during formation. The TOC content is highest in both peaty horizons, reaching up to 9 wt% in the upper peaty horizon. Furthermore, TOC/TN values are highest (up to 22) while  $\delta^{13}\text{C}$  values are lowest ( $-29.3$  to  $-26.1\text{\textperthousand}$ ) in both peaty horizons. A smaller degree of organic matter decomposition within the peaty horizons is indicated by these data. The stable isotope composition of segregation ice ranges widely, between  $-32.3$  and  $-21.5\text{\textperthousand}$  for  $\delta^{18}\text{O}$  and between  $-246.3$  and  $-178.6\text{\textperthousand}$  for  $\delta\text{D}$ . The d excess varies between  $-6.7$  and  $19.4$  (Fig. 4a). Increasing (less negative) values of  $\delta^{18}\text{O}$  and  $\delta\text{D}$  are observed towards both peaty horizons while d excess values decrease. The overall correlation as expressed in a  $\delta^{18}\text{O}$ - $\delta\text{D}$  bi-plot is good ( $r^2 = 0.98$ ); the slope is 5.9 ( $\delta\text{D} = 5.92 * \delta^{18}\text{O} - 49.97$ ) and the regression line crosses the Global Meteoric Water Line (GMWL, Fig. 6).

Ice-wedge stable water isotopes are commonly used as a proxy for winter air temperature (e.g. Meyer et al., 2010, 2015) where more negative (isotopically depleted) values reflect colder conditions and less negative values reflect warmer conditions. The mean stable water isotope values of the L7-15 syngenetic ice wedge transect ( $n = 9$ ) are  $-33.0\text{\textperthousand}$  for  $\delta^{18}\text{O}$ ,  $-257.2\text{\textperthousand}$  for  $\delta\text{D}$ , and 7‰ for d excess. The respective minima and maxima vary little, between  $-33.6$  and  $-32.6\text{\textperthousand}$  for  $\delta^{18}\text{O}$ ,  $-260.4$  and  $-253.7\text{\textperthousand}$  for  $\delta\text{D}$ , and 6 and 8‰ for d excess. The slope in a  $\delta^{18}\text{O}$ - $\delta\text{D}$  bi-plot is 6.9

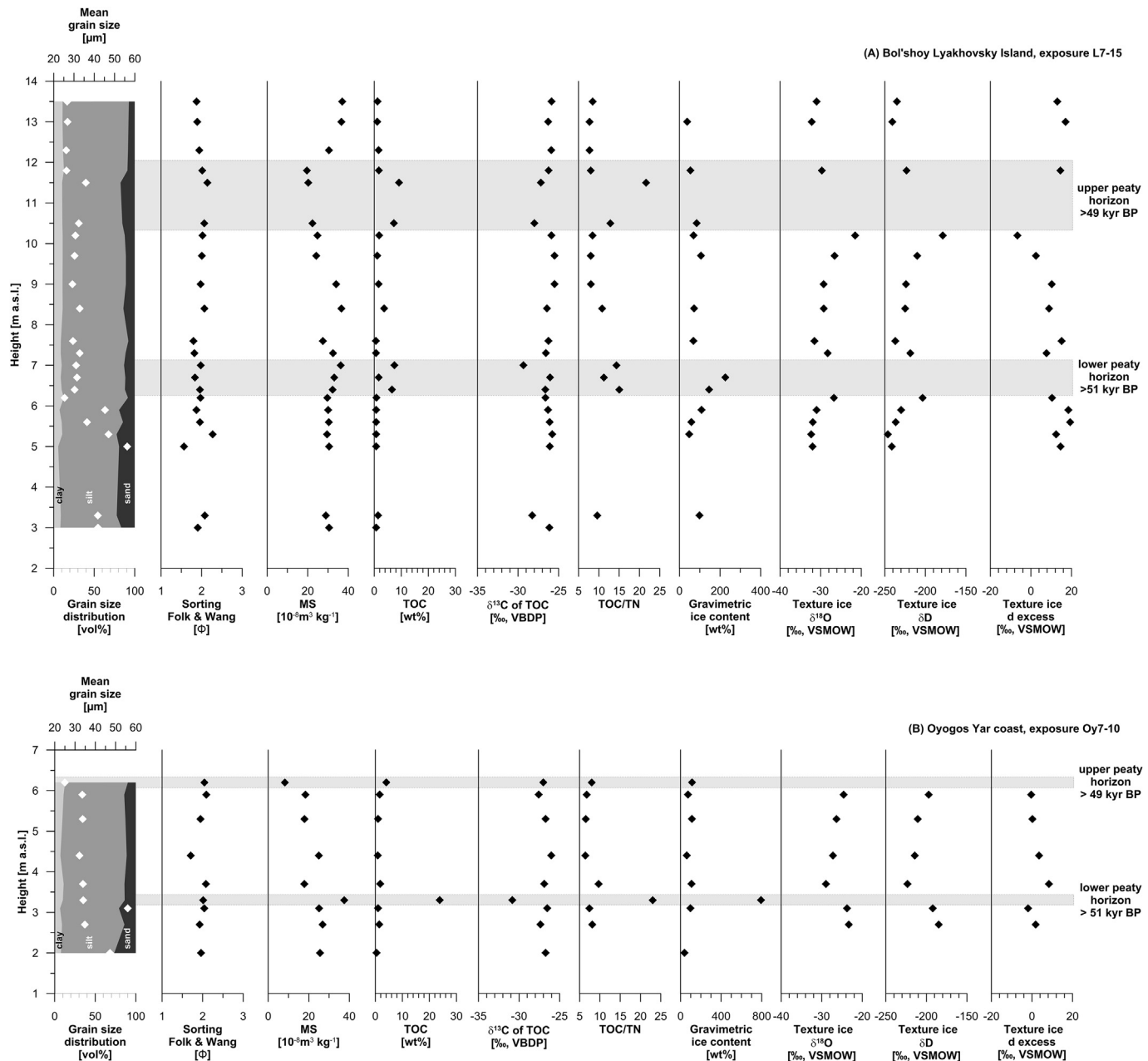


Fig. 4. Cryolithological properties of (A) profile L7-15 (Bol'shoy Lyakhovsky Island) and (B) profile Oy7-10 (Oyogos Yar coast).

( $\delta\text{D} = 6.9 * \delta^{18}\text{O} - 29$ ) and the correlation coefficient  $r^2 = 0.99$  (Fig. 6).

The Buchchagy IC profile on the Oyogos Yar mainland coast (Oy7-10) is demarcated by two syngenetic ice wedges several metres wide (Fig. 3). Below the lower peaty horizon (between about 2 and 3 m a.s.l.), the deposits are composed of brown silt with ice bands (0.5–1 cm thick, 4–6 cm apart) and a lens-like layered cryostructure. The ice content reaches 97 wt%. The lower peaty horizon is represented by one sample at 3.3 m a.s.l. (Fig. 3) of brown peat in a matrix of grey silt with ice bands and lens-like reticulated cryostructures. The ice content of 794 wt% indicates high ice oversaturation. The deposits overlying the lower peaty horizon (between 3.5 and 6 m a.s.l.) are grey-brown silts with lens-like and reticulated cryostructures between ice bands (0.5–2 cm thick, 5–10 cm apart). The ice content varies between 61 and 112 wt%. The

upper peaty horizon, sampled at 6.2 m a.s.l., represents the uppermost sample of the Oy7-10 profile. Its cryostructures are the same as those below and the ice content is 113 wt%. In general, the Oy7-10 profile resembles the cryolithological properties of the L7-15 profile on a smaller scale and at a lower sampling resolution (Fig. 4b). The granulometrical composition of the Oy7-10 deposits is almost the same as that of the L7-15 deposits (Fig. 5b). The MS is highest (37.5 SI) in the lower peaty horizon and lowest (8.2 SI) in the upper peaty horizon. The Oy7-10 organic matter properties are comparable to those of the L7-15 profile with increased TOC and TOC/TN and decreased  $\delta^{13}\text{C}$  values, especially in the lower peaty horizon.

The stable water isotope values of segregation ice of Oy7-10 show less variation if compared to L7-15 data, between  $-29.0$  and  $-23.3\text{\textperthousand}$  for  $\delta^{18}\text{O}$ , and  $-223.3$  and  $-184.7\text{\textperthousand}$  for  $\delta\text{D}$ . The d excess

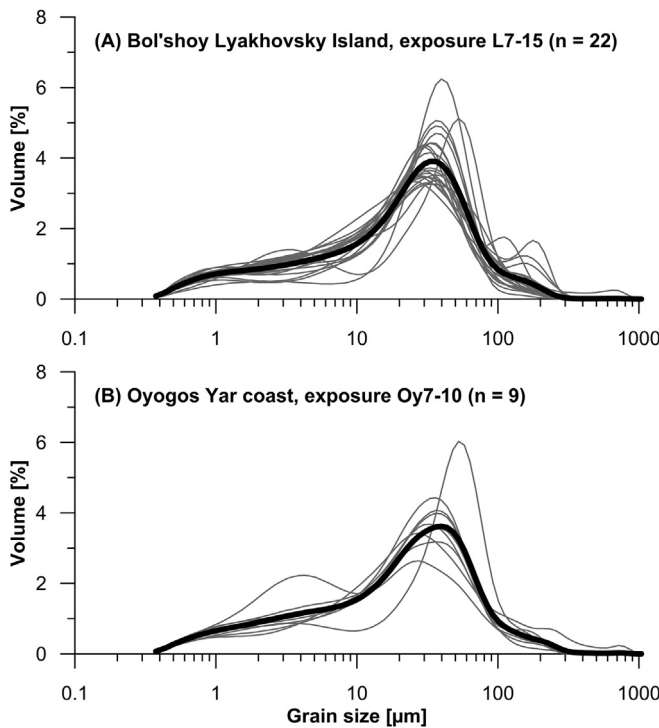


**Fig. 5.** Grain size distribution curves of (A) profile L7-15 (Bol'shoy Lyakhovsky Island) and (B) profile Oy7-10 (Oyogos Yar coast).

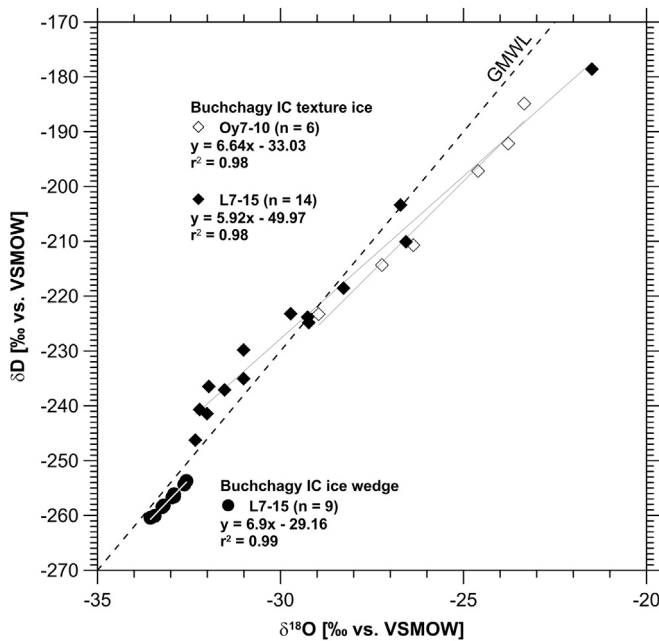


**Fig. 6.** Co-isotopic cross plot ( $\delta^{18}\text{O}$ ,  $\delta\text{D}$ ) of Buchchagy ground ice in profiles L7-15 and Oy7-10.

varies between  $-1.9$  and  $8\text{‰}$  (Fig. 4b). However, increasing (less negative) values of  $\delta^{18}\text{O}$  and  $\delta\text{D}$  and decreasing d excess values are again notable from the lower to the upper peaty horizons. The overall correlation as expressed in a  $\delta^{18}\text{O}$ - $\delta\text{D}$  bi-plot is good ( $r^2 = 0.98$ ); the slope is  $6.64$  ( $\delta\text{D} = 6.6 \cdot \delta^{18}\text{O} - 33$ ) (Fig. 6).

#### 4.2. Dating

In order to provide a chronological evaluation of the Buchchagy IC formation, AMS radiocarbon dating and  $^{230}\text{Th}/\text{U}$  radioisotope dating were applied to material from both peaty horizons. Undeterminable fossil plant fragments from both peaty horizons of the L7-15 and Oy7-10 profiles were radiocarbon dated. Samples of the lower peaty horizons from both studied profiles gave non-finite radiocarbon dates of  $>51$  kyr BP, while samples from the upper peaty horizons from both studied profiles gave non-finite radiocarbon dates of  $>49$  kyr BP (Table 1). The non-finite ages of the dated peaty horizons clearly indicate pre-MIS3 formation of the Buchchagy IC, which thus predates the Yedoma IC.

Both Buchchagy peaty horizons exposed at Bol'shoy Lyakhovsky Island were radioisotopically dated by  $^{230}\text{Th}/\text{U}$  (Tumskoy, 2009). The radioisotope disequilibria results from the lower peaty horizon of profile L7-15 are given in Fig. 7 and Table 2. A linear dependence with correlation coefficients of better than 0.99 in the isochronous coordinates is found for three out of five sub-samples (LUU-341, LUU-342, LUU-343). Two other samples (LUU-340, LUU-344) do not fit on the isochronous lines and were excluded from age calculation (Fig. 7). Based on the good agreement between isochronously corrected ages, the lower peaty horizon of the L7-15 profile has been dated according to a linear calculating technique (Maksimov and Kuznetsov, 2010) by the L/L model to  $117 + 19/-14$  kyr (136–103 kyr), while the TSD model gave an age of  $126 + 16/-13$  kyr (142–113 kyr). The overlapping age interval and the deduced formation age of the lower peaty horizon of the Buchchagy IC is 136 to 113 kyr. Because the upper peaty horizon of the L7-15 profile could not be dated due to sample loss during transportation from the field to the laboratory, previous  $^{230}\text{Th}/\text{U}$  radioisotope dating results of the upper peaty horizon are employed here (Tumskoy, 2009; Tumskoy et al., under review). The upper peaty horizon of the Buchchagy IC was sampled in 2004 at the southern coast of Bol'shoy Lyakhovsky Island. Tumskoy et al. (under review) describe further details on age deduction by linear and non-linear approaches of  $^{230}\text{Th}/\text{U}$  analyses. The upper Buchchagy peaty horizon of the Buchchagy IC (sample ID JL102) was dated by the best-fitting non-linear approach to  $93 + 5/-5$  kyr (98–88 kyr; L/L model) and to  $89 + 5/-5$  kyr (94–84 kyr; TSD model). The overlapping age interval and the deduced formation age of the upper peaty horizon of the Buchchagy IC is 94 to 88 kyr.

Based on these chronological data the formation of the Buchchagy IC including both characteristic peaty horizons during MIS5e-5b is assumed.

#### 4.3. Pollen and NPP stratigraphy

The pollen assemblages of the L7-15 profile (Fig. 8) are subdivided into six PZs.

PZ-I (3–3.5 m a.s.l.) contains only two samples with very distinct pollen spectra. Poaceae and Cyperaceae pollen dominate the lowermost sample (3.0 m a.s.l.). Arboreal pollen (AP) is represented by non-identifiable Pinaceae, *Pinus* and *Picea*, but generally, the AP percentages are very low (ca. 5%). Poaceae almost completely dominate the upper spectrum of PZ-I at 3.3 m a.s.l. Both samples belong to the Kuchchugui stratum (Fig. 2).

PZ-II (5–6.3 m a.s.l.) is notable for very high percentages of AP (up to 48%) represented by the relatively well-preserved pollen of conifers (mostly *Picea* with numerous *Pinus*, *Abies*, and *Larix*). Pinaceae pollen appears to be partly redeposited (redep. in Figs. 8 and 9) from the older sediments and is marked in the diagram as Pinaceae spp. These grains are mostly indeterminable and differ from younger pollen grains by their darker colour, different auto-fluorescence, and exine raptures. Pollen of *Betula* spp. and *Alnus*

**Table 1**

Radiocarbon dates of the upper and lower Buchchagy Ice Complex peaty horizons probed in profile L7-15 (Bol'shoy Lyakhovsky Island) and profile Oy7-10 (Oyogos Yar coast) on Dmitry Laptev Strait coasts.

Sample N°	Lab N°	Material	Height [m a.s.l.]	Radiocarbon ages [ $^{14}\text{C}$ yr BP]	Remarks
<b>Bol'shoy Lyakhovsky Island</b>					
L7-15-06	Poz-48075	Indeterminable plant fragments	10.5	>49,000	Upper peat
L7-15-15	Poz-48074	Indeterminable plant fragments	7	>51,000	Lower peat
<b>Oyogos Yar mainland coast</b>					
Oy7-10-09	Poz-51638	Indeterminable plant fragments	6.2	>49,000	Upper peat
Oy7-10-04	Poz-51637	Indeterminable plant fragments	3.3	>51,000	Lower peat

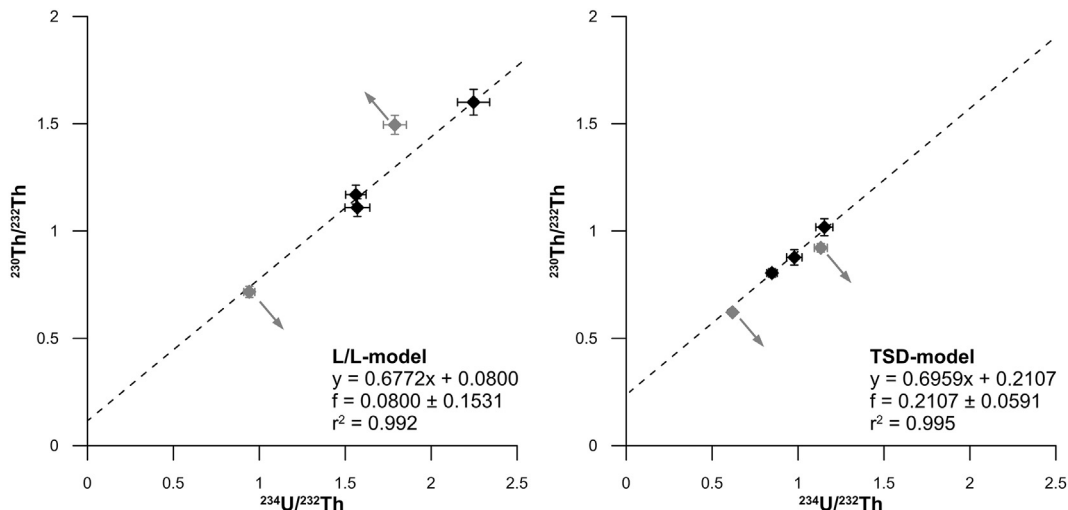


**Fig. 7.** Radiochemical ratios ( $^{230}\text{Th}/^{232}\text{Th}$  vs.  $^{234}\text{U}/^{232}\text{Th}$ ) of five sub-samples from the lower peaty horizon of profile L7-15 (Buchchagy Ice Complex, Bol'shoy Lyakhovsky Island) determined by applying the L/L model (left plot) and the TSD model (right plot). Grey diamonds indicate data not included in the radioisotope disequilibrium age determination.

**Table 2**

Radiochemical properties of five sub-samples from the lower peaty horizon of profile L7-15 (Buchchagy Ice Complex, Bol'shoy Lyakhovsky Island) determined by applying the leachate alone technique (L/L model) and the total sample dissolution technique (TSD model) after Maksimov and Kuznetsov (2010). Units of  $\text{dpm g}^{-1}$  refer to decay per minute per gram.

N° LUU	Ash [%]	$^{238}\text{U}$ [ $\text{dpm g}^{-1}$ ]	$^{234}\text{U}$ [ $\text{dpm g}^{-1}$ ]	$^{230}\text{Th}$ [ $\text{dpm g}^{-1}$ ]	$^{232}\text{Th}$ [ $\text{dpm g}^{-1}$ ]	$\frac{^{230}\text{Th}}{^{234}\text{U}}$	$\frac{^{234}\text{U}}{^{238}\text{U}}$	$\frac{^{230}\text{Th}}{^{232}\text{Th}}$	$\frac{^{234}\text{U}}{^{232}\text{Th}}$
<b>L/L-technique</b>									
340	86.9	$0.275 \pm 0.007$	$0.323 \pm 0.008$	$0.246 \pm 0.007$	$0.343 \pm 0.008$	$0.761 \pm 0.029$	$1.176 \pm 0.039$	$0.717 \pm 0.026$	$0.942 \pm 0.032$
341	62.8	$0.648 \pm 0.026$	$0.749 \pm 0.028$	$0.529 \pm 0.014$	$0.477 \pm 0.013$	$0.706 \pm 0.032$	$1.155 \pm 0.051$	$1.109 \pm 0.041$	$1.571 \pm 0.072$
342	51.1	$0.777 \pm 0.024$	$0.919 \pm 0.027$	$0.655 \pm 0.015$	$0.409 \pm 0.012$	$0.712 \pm 0.027$	$1.183 \pm 0.038$	$1.600 \pm 0.060$	$2.247 \pm 0.094$
343	66.1	$0.708 \pm 0.020$	$0.838 \pm 0.022$	$0.628 \pm 0.016$	$0.537 \pm 0.015$	$0.749 \pm 0.028$	$1.184 \pm 0.035$	$1.170 \pm 0.044$	$1.562 \pm 0.059$
344	54.1	$0.695 \pm 0.022$	$0.816 \pm 0.024$	$0.682 \pm 0.013$	$0.456 \pm 0.010$	$0.836 \pm 0.029$	$1.174 \pm 0.039$	$1.495 \pm 0.044$	$1.789 \pm 0.067$
<b>TSD-technique</b>									
340t	86.9	$1.411 \pm 0.033$	$1.463 \pm 0.034$	$1.470 \pm 0.024$	$2.364 \pm 0.032$	$1.005 \pm 0.029$	$1.037 \pm 0.029$	$0.622 \pm 0.013$	$0.619 \pm 0.017$
341t	62.8	$1.558 \pm 0.050$	$1.614 \pm 0.051$	$1.531 \pm 0.028$	$1.902 \pm 0.031$	$0.949 \pm 0.035$	$1.035 \pm 0.037$	$0.805 \pm 0.019$	$0.848 \pm 0.030$
342t	51.1	$1.459 \pm 0.049$	$1.573 \pm 0.052$	$1.389 \pm 0.038$	$1.364 \pm 0.038$	$0.883 \pm 0.038$	$1.078 \pm 0.040$	$1.018 \pm 0.040$	$1.153 \pm 0.050$
343t	66.1	$1.466 \pm 0.054$	$1.579 \pm 0.057$	$1.416 \pm 0.042$	$1.614 \pm 0.045$	$0.897 \pm 0.042$	$1.077 \pm 0.046$	$0.877 \pm 0.036$	$0.978 \pm 0.045$
344t	54.1	$1.358 \pm 0.043$	$1.593 \pm 0.048$	$1.297 \pm 0.020$	$1.407 \pm 0.021$	$0.814 \pm 0.027$	$1.173 \pm 0.040$	$0.922 \pm 0.020$	$1.132 \pm 0.038$

*fruticosa* type (also known as *Duschekia fruticosa* and *Alnaster*) prevail among deciduous taxa. Ericales pollen is also constantly present in PZ-II. Poaceae and Cyperaceae dominate the non-arbooreal pollen (NAP). Herbs are represented by Asteraceae, *Artemisia*, Ranunculaceae, Chenopodiaceae, Rosaceae, etc. Among spores, Polypodiophyta, *Sphagnum*, and *Lycopodium* have significant abundances. *Selaginella rupestris* and *Huperzia* are not abundant, and occur only in this zone. Dominating NPPs are *Zygnuma*, *Glomus*, and remains of *Botryococcus* colonies.

PZ-III (6.3–7.1 m a.s.l.) is characterised by a sharp decrease of AP contents (mostly conifers) and an increase in pollen concentration. Ericales pollen is present in two samples. Among NAP, abundances of Poaceae and Cyperaceae increase. Abundances of Asteroideae,

Ranunculaceae, and Papaveraceae also slightly increase in PZ-III. Spores are represented by Polypodiophyta and *Lycopodium*. The composition of NPPs is similar to that found in PZ-II. The PZ-III composition corresponds to that of the lower peaty horizon of profile L7-15.

The two samples of PZ-IV (7.1–8.1 m a.s.l.) are distinguished by higher AP percentages (46 and 61%). Much of the AP consists of coniferous pollen. Abundances of *Picea*, *Pinus*, *Abies*, and *Larix* pollen are the highest in the profile. Other AP belongs to *Betula*, *A. fruticosa*, and *Salix*. Single grains of cf. *Carpinus* were also found in PZ-IV. Ericales percentages reach ca. 2% in this PZ. Cyperaceae and Poaceae dominate the NAP. In the lower sample of PZ-IV at 7.3 m a.s.l., single pollen grains of aquatic plants (*Typha*, *Nuphar*)

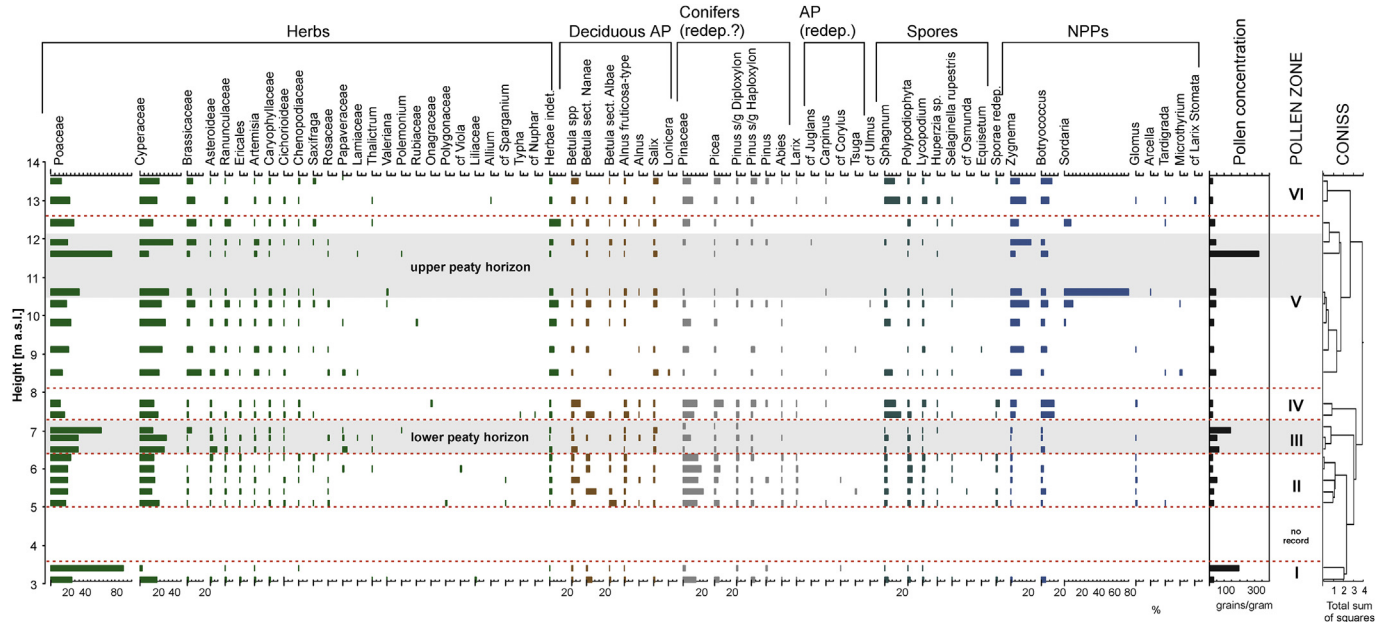


Fig. 8. Palynological results from profile L7-15 (Bol'shoy Lyakhovsky Island).

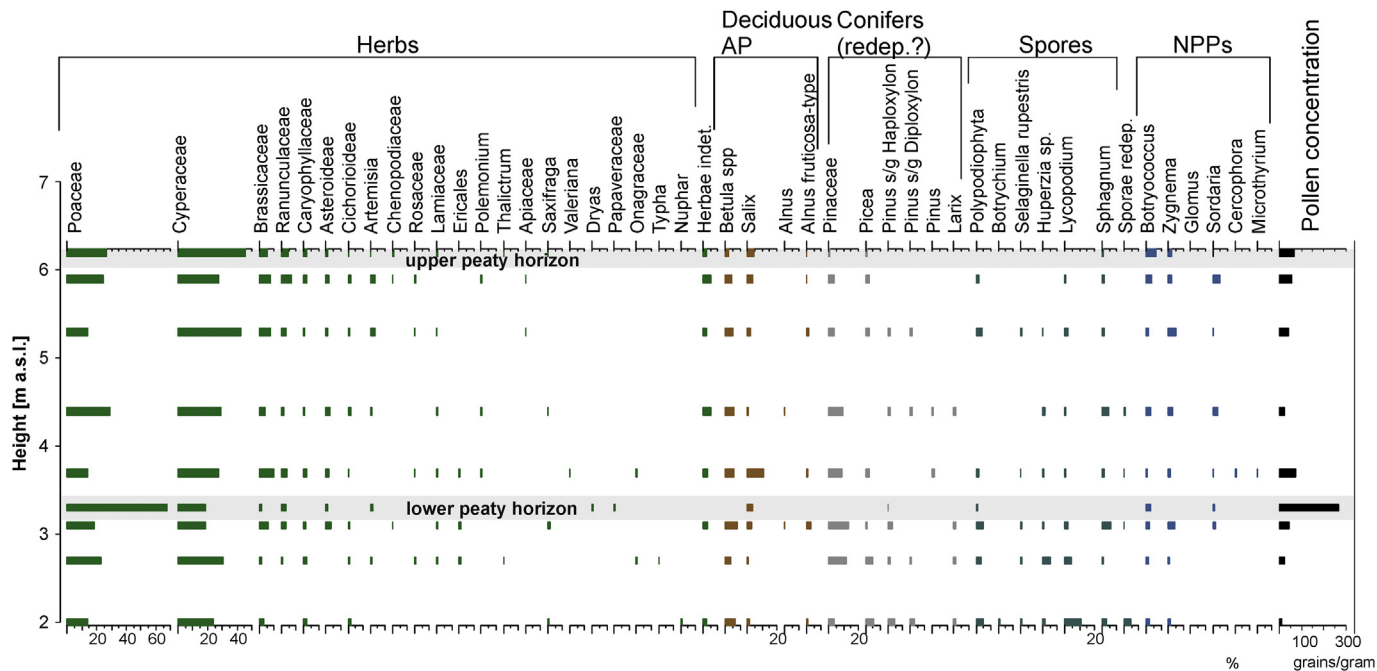


Fig. 9. Palynological results from profile Oy7-10 (Oyogos Yar coast).

were found. Spores are represented mostly by Polypodiophyta, *Sphagnum*, and *Lycopodium*. Remains of *Botryococcus* and spores of *Zygnema* are abundant among the NPPs.

The AP percentages sharply decrease in PZ-V (8.1–12.5 m a.s.l.), while pollen concentration increases slightly. Cyperaceae and Poaceae dominate among NAP; abundances of herbaceous pollen like Brassicaceae, Asteraceae (including *Artemisia*), Ranunculaceae, and Caryophyllaceae increase significantly. AP is represented by conifers, *Betula* and *Salix*. *Salix* pollen content slightly increases in this zone. Single pollen grains of probably redeposited cf. *Carpinus* and cf. *Ulmus* were found in several samples of PZ-V. Spore findings

belong to Polypodiophyta, *Lycopodium* sp., and *S. rupestris*. *Zygnema* spores prevail in the NPPs. Three upper samples between 10.5 and 11.8 m a.s.l. represent the upper L7-15 peaty horizon. However, the pollen spectra fit well in the PZ-V description and therefore the upper peaty horizon is not distinguished from other PZ-V pollen assemblages.

The PZ-VI pollen composition (12.5–13.5 m a.s.l.) is similar to that found in PZ-V. Distinctive features of PZ-VI are the near absence of Ericales, the presence of *Huperzia*, and single grains of *Larix* and *Larix*-type stomata in one of the upper samples. Spores of *Sphagnum* significantly increase in PZ-VI.

The Oy7-10 pollen complex is characterised by the dominance of Poaceae and Cyperaceae in line with the L7-15 pollen record. Any differentiation into single PZs is not obvious. Other dominant herbaceous taxa are Brassicaceae, Ranunculaceae, Caryophyllaceae, and Asteraceae. *Betula* and *Salix* pollen are significantly abundant in the Oy7-10 pollen spectra. Among conifers, *Picea* and *Pinus* spp. pollen is relatively well preserved; however, most coniferous pollen appear to have been reworked (Pinaceae spp. on the pollen diagram; Fig. 9). The lower peat sample (3.3 m a.s.l.) shows very high Poaceae pollen percentages, rare AP and conifers, and a relatively high pollen concentration. The upper peat sample (6.2 m a.s.l.) is not distinguished from other pollen spectra.

## 5. Discussion

### 5.1. Formation, degradation, and preservation of the MIS5 Buchchagy Ice Complex

Remnants of the Buchchagy IC are preserved, in places, over tens of kilometres along both coastlines of the Dmitry Laptev Strait and therefore assessed to be of regional stratigraphic relevance (Tumskoy and Dobrynin, 2008). The formation of the Buchchagy IC during MIS5 *sensu lato* and its persistence since then indicate non-glacial environments in the study region at least during the last glacial cycle (Fig. 1a; Möller et al., 2015). Late Pleistocene glaciations never reached the East Siberian arctic lowlands and the adjacent shelf (Elias and Brigham-Grette, 2013). The Buchchagy IC is recognised by its stratigraphic position below the Yedoma IC and the characteristic presence of large ice wedges and two peaty horizons within the sediment (Fig. 1). Based on the records presented here, the formation of Buchchagy IC deposits is assumed to be similar to the Yedoma IC (Schirrmeister et al., 2011a, 2013). Past polygon tundra environments with diverse sediment supply by alluvial and aeolian transport as well as on-site peat growth promoted the accumulation of the Buchchagy IC, which were then superimposed by intense syngenetic ice-wedge growth. Typical cryostructures of ice bands and lens-like ice between the bands point to long term stable surface. Ice wedge dimensions and high ice contents indicate that there was sufficient moisture supply by precipitation to feed the ground ice. The large percentage of ground ice within the Buchchagy IC, however, made it highly vulnerable to thaw during warmer periods of possibly the MIS5 and the lateglacial-Holocene warming.

### 5.2. Comparison of the MIS5 Buchchagy Ice Complex to the MIS3–MIS2 Yedoma Ice Complex

The narrow range of the ice-wedge stable isotope data indicates cold and stable winter conditions during ice-wedge formation. The mean  $\delta^{18}\text{O}$  values of  $-33\text{\textperthousand}$  are about  $2\text{\textperthousand}$  lower than that of the Molotkov interstadial (MIS3) ice wedges (Meyer et al., 2002; Wetterich et al., 2014) and confirm colder winter temperatures during formation of the Buchchagy IC (MIS5e–b) (Fig. 10). However, the  $\delta^{18}\text{O}$  values of the Sartan Stadial (MIS2) are about  $4\text{\textperthousand}$  more depleted and represent the coldest winter conditions observed so far in the study region (Wetterich et al., 2011). The slope of 6.9 in a  $\delta^{18}\text{O}$ – $\delta\text{D}$  co-isotope plot ( $n = 9$ ) as well as the mean d excess value of 6.7 fit well to that of the MIS2 stadial ice wedges (Wetterich et al., 2011) and point to similar general atmospheric circulation dynamics that are slightly different than interstadial (i.e. MIS3) conditions (Wetterich et al., 2014). Cold continental wintertime conditions are assumed for the time of the Buchchagy IC formation.

The segregation ice stable water isotope data for both the Bol'shoy Lyakhovsky and Oyogos Yar study sites display a wide scatter (Fig. 4), indicating that different water sources (e.g. rain, snow,

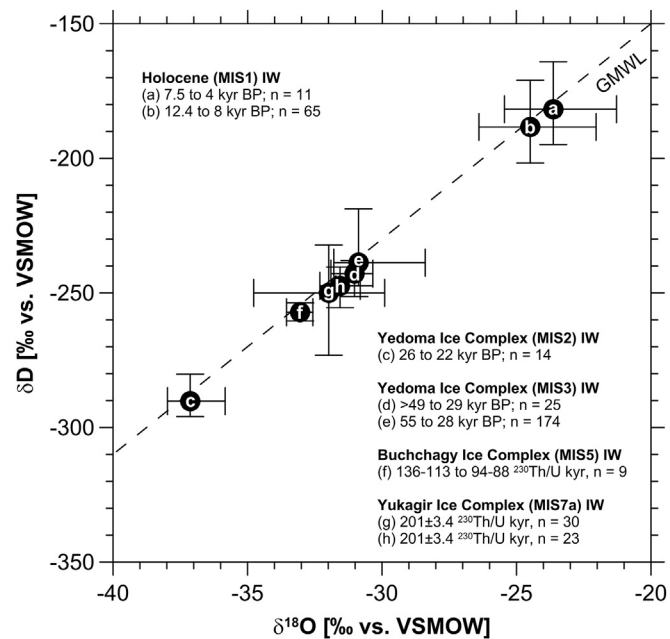


**Fig. 10.** Cross-plot compilation of stable-water isotope data ( $\delta^{18}\text{O}$ ,  $\delta\text{D}$ ) in several generations of syngenetic ice wedges (IW) exposed at the southern coast of Bol'shoy Lyakhovsky Island. Ice-wedge data sources: Holocene (MIS1) (Meyer et al., 2002; Wetterich et al., 2009); Yedoma Ice Complex (MIS2) (Wetterich et al., 2011); Yedoma Ice Complex (MIS3) (Meyer et al., 2002; Wetterich et al., 2014); Buchchagy Ice Complex (MIS5) (this study); Yukagir Ice Complex (MIS7a) (Meyer et al., 2002).

ground-ice melt water) and several fractionation processes (e.g. freeze–thaw cycles, evaporation) in the active layer were involved prior to final ice formation. The slopes of 5.9 ( $n = 14$ ) and 6.6 ( $n = 6$ ) for Bol'shoy Lyakhovsky and Oyogos Yar, respectively, in  $\delta^{18}\text{O}$ – $\delta\text{D}$  co-isotope plots are comparable to those previously reported for Yedoma IC segregation ice (5.2 and 6.5; Wetterich et al., 2014 and Meyer et al., 2002, respectively), pointing to substantial secondary fractionation processes. Hence, the stable water isotope composition indicates ice formation conditions rather than climate signals. Distinct trends of isotopic enrichment ( $\delta^{18}\text{O}$  and  $\delta\text{D}$ ) and d excess decrease towards the peaty horizons are the most remarkable features in the records (Fig. 4). Together with the  $\delta^{18}\text{O}$ – $\delta\text{D}$  slopes that are close to a freezing slope, this might point to isotopic fractionation during downward directed sediment-freezing processes under more-or-less closed-system conditions as interpreted also for MIS3 segregation ice (Wetterich et al., 2014).

The palynological study of the L7-15 profile suggests that PZ-I represents the Kuchchugui stratum. The upper part of L7-15 and the entire Oy7-10 profiles are assigned to the Bychchagy IC that is characterised by two distinct peaty horizons.

Generally, pollen records of the Kuchchugui stratum from the Laptev Sea region are characterised by relatively low pollen concentration, high contents of Asteroideae and Cichorioideae, and large amounts of reworked Pinaceae pollen (Andreev et al., 2011 and references therein). The presence of green algae and spores of coprophilous Sordariales reflect the presence of freshwater pools and large mammal grazers, respectively. Pollen assemblages of the Kuchchugui stratum described by Barkova (1982) from Oyogos Yar and by Andreev et al. (2004) from Bol'shoy Lyakhovsky Island are rather similar (including the large amounts of coniferous pollen). However, Barkova (1982) considers this pollen assemblage to be evidence of forest vegetation development during the formation of the Kuchchugui stratum, and Andreev et al. (2004) interpret this conifer pollen as reworked. Following Andreev et al. (2004),

numerous Pinaceae pollen (Pinaceae spp. in Figs. 8 and 9) in the L7-15 and Oy7-10 spectra are considered to be reworked. The high contents of reworked material probably indicate a scarce vegetation cover with low pollen production as well as active erosion in the region (Andreev et al., 2011). In this case, the pollen concentration is low in general and reworked pollen percentages are higher in the total pollen sum. Coniferous pollen from mid- and late-Pleistocene records of Bol'shoy Lyakhovsky Island and Oyogos Yar is mostly redeposited from older Cenozoic sediments. This is indirectly confirmed by the presence of broad-leaved tree pollen in the L7-15 spectra. Thus, we suggest that high abundances of coniferous pollen and low pollen concentration in the sediments are evidence of scarce vegetation due to harsh climate and erosion during the formation of the Kuchchugui stratum.

Pollen spectra of the Bychchagy IC deposits (PZ-II to PZ-VI of L7-15 and Oy7-10 records) reflect environmental changes. Pollen assemblages coinciding with peat accumulation (lower and upper peaty horizons) were formed under a milder climate, suggested by higher pollen concentration, high abundances of grass and sedge pollen, and the rare presence of reworked coniferous pollen. Sediments that accumulated before (PZ-II of L715) and after (PZ-IV of L7-15) the formation of the lower Buchchagy IC are characterised by high percentages of reworked conifers and low diversity of forbs pollen taxa. Climate was presumably the harshest throughout the time of accumulation. The significant increase in the remains of algae (*Botryococcus* and *Zygnum*) reflects sedimentation in shallow-water conditions (at least seasonally). The L7-15 PZ-V pollen assemblages, with relatively high abundances of *Artemisia* and high diversity of other herbaceous taxa, resemble tundra and steppe vegetation. The high amounts of coprophilous *Sordaria* in this PZ indirectly point to the presence of grazing animals, also confirming more favourable environmental conditions. The uppermost L7-15 PZ-VI resembles PZ-IV that overlies the lower peaty horizon and could have been formed under similar harsh environmental conditions. Remnants of *Zygnum* and *Botryococcus* that appeared in significant amounts in PZ-IV, PZ-V, and PZ-VI of the L7-15 profile can be interpreted as evidence for shallow-water habitats (namely polygon ponds) at the studied site (de Klerk et al., 2014).

Generally, the pollen records of the Buchchagy IC are comparable to previously studied pollen records from younger Yedoma IC deposits on Bol'shoy Lyakhovsky Island (Andreev et al., 2009, 2011; Wetterich et al., 2011, 2014). Changing vegetation of tundra-steppe communities is recorded on millennial time scales. In this context, the MIS5 Buchchagy pollen record documents harsher environmental conditions than during the MIS3 interstadial and rather similar conditions as during MIS2. This is reflected in a lower pollen concentration and a small amount of redeposited arboreal tree pollen (Pinaceae, Betula) in pollen records of the Buchchagy IC. High percentages of Brassicaceae in the Buchchagy IC (MIS5) pollen spectra are typical if compared to MIS3 pollen records, where Caryophyllaceae ranks third in abundance of herbaceous taxa (Wetterich et al., 2014). This feature indirectly confirms the deduced harsher climate during MIS5 because Brassicaceae is more typical today of high Arctic vegetation than Caryophyllaceae (Tolmachev [ed.], 1971, 1975). A MIS2 pollen record from Bol'shoy Lyakhovsky Island (Wetterich et al., 2011) reveals higher abundances of *Artemisia* pollen than in MIS3 and MIS5 spectra. Interpreting *Artemisia* as indicating dry conditions, we assume more humid climate conditions during MIS5 and MIS3 than during MIS2.

### 5.3. Chronostratigraphy and lithostratigraphy of the MIS5 Buchchagy Ice Complex

When using permafrost as a paleoenvironmental archive, several limitations have to be taken into account. Most prominent

is the frequent lack of continuous permafrost sequences due to the intense and varying landscape history of thermally-induced sediment erosion and relocation (thermokarst) during warm stages, and other ongoing erosion processes. Consequently, local stratigraphy is sometimes difficult to correlate on regional scale. Despite the wide use of different geochronological methods on permafrost such as radiocarbon dating (e.g. Vasil'chuk and Vasil'chuk, 2014), optically- and infrared-stimulated luminescence (OSL and IRSL; e.g. Krubetschek et al., 2000; Andreev et al., 2004; Schirmeister et al., 2010, 2011c), thermo-luminescence (TL; e.g. Arkhangelov et al., 1996),  $^{230}\text{Th}/\text{U}$  radioisotope disequilibrium of frozen peat (Schirmeister et al., 2002; Wetterich et al., 2008), or ground ice  $^{36}\text{Cl}/\text{Cl}$  radionuclide ratios (Gilichinsky et al., 2007; Tikhomirov and Blinov, 2009; Blinov et al., 2009), there are still large uncertainties when comparing different geochronological results. Some uncertainties are probably related to unknown influences of permafrost processes on chemical and physical parameters important to the age determination techniques. Ewing et al. (2015) evaluated in a novel approach the use of radioactive disequilibrium among uranium isotopes in thaw water to estimate the age of intra-sedimentary syngenetic ground ice in Alaskan loess. Developing dating techniques and increasing understanding of controlling periglacial processes allow for improved chronostratigraphies of permafrost sequences.

The formation age and stratigraphic context of the Buchchagy IC are deduced using several approaches. The stratigraphic position of Buchchagy IC exposures below the Yedoma IC (Fig. 1) is in agreement with non-finite radiocarbon dates of both peaty horizons of profiles L7-15 and Oy7-10 (Table 1). A minimum deposition age for the Buchchagy IC of older than MIS3 is therefore assumed. The  $^{230}\text{Th}/\text{U}$  dates of the Buchchagy IC peaty horizons of  $126 + 16/-13$  kyr and  $117 + 19/-14$  kyr (lower peaty horizon) and of  $98 \pm 5$  kyr and  $89 \pm 5$  kyr (upper peaty horizon) confirm a formation of this IC during MIS5e-5b.

Using cosmogenic nuclides preserved in ice-wedges of the Buchchagy IC as a dating tool was first applied by Blinov et al. (2009). The  $^{36}\text{Cl}/\text{Cl}$  dating failed at samples from profile L7-15, but revealed ages for Oy7-03-101 IW of  $68 \pm 31$   $^{36}\text{Cl}/\text{Cl}$  kyr and Oy7-03-201 IW of  $98 \pm 31$   $^{36}\text{Cl}/\text{Cl}$  kyr from ice wedges, which are attributed to the Buchchagy IC (Blinov et al., 2009). The ice-wedge-based median base age in Oy7-03-101 IW is younger than expected, but the rather broad minimum–maximum age range indicated falls at least in the  $^{230}\text{Th}/\text{U}$  age range. Blinov et al. (2009) propose influences on the age determination by fractionation of the chlorine isotope ratio in the water phase during transport from the surface to ice wedges due to evaporation, condensation and/or chemical binding. Post-depositional lateral ion exchange between ice and the surrounding frozen sediment along concentration gradients, as well as partial ground-ice melt, might also alter the  $^{36}\text{Cl}/\text{Cl}$  ages. The  $^{36}\text{Cl}/\text{Cl}$  age of Oy7-03-201 IW coincides with the  $^{230}\text{Th}/\text{U}$  age of the Buchchagy IC and is interpreted as additional evidence of the assumed IC formation during MIS5 *sensu lato*.

Tumskoy (2009, 2012) proposes that the lithostratigraphic position of the Buchchagy IC is older than the Last Interglacial. Consequently, the numerous exposures of Last Interglacial ice-wedge casts along both coasts of the Dmitry Laptev Strait formed by ground ice melt of ice wedges of the Buchchagy IC and promoted further permafrost degradation (Ivanov, 1972). Several palaeoecological studies on Last Interglacial lacustrine deposits (Andreev et al., 2004; Ilyashuk et al., 2006; Kienast et al., 2008; Wetterich et al., 2009) point to continental inland conditions and temperatures in the warmest month that were  $10^{\circ}\text{C}$  warmer than today ( $T_{\text{July}} > 13^{\circ}\text{C}$ , Kienast et al., 2011). Such warm summer conditions explain widespread and intense thermokarst development that degraded underlying ice-rich deposits. However, the

chronostratigraphical context between the Last Interglacial and the Buchchagy IC is still complicated by the lack of direct Last Interglacial deposit age determinations. Two IRSL dates from taberite deposits underlying a Last Interglacial ice wedge cast on Bol'shoy Lyakhovsky Island (section R22\_60 in Andreev et al., 2004) provide ages of  $99 \pm 15$  kyr and  $102 \pm 16$  kyr. Andreev et al. (2004) assume a "relatively good agreement with a suggested Eemian age for the ice-wedge cast" and explain these young ages by thaw during thermokarst formation and later re-freezing, which altered physical and chemical properties of the material and consequently the deduced IRSL ages. Hitherto, other than TL dating of lacustrine deposits from Bol'shoy Lyakhovsky Island to  $136 \pm 34$  kyr (Arkhangelov et al., 1996), direct age indications for the Last Interglacial are not available. Due to the uncertainties in chronostratigraphy and regional timing of the Last Interglacial, the lithostratigraphic contact between the Buchchagy IC and Last Interglacial thermokarst still needs clarification. As proposed by Tumskoy (2012), the ice-rich Buchchagy IC might have been the material that degraded largely during the Last Interglacial. Based on the Buchchagy IC  $^{230}\text{Th}/\text{U}$  dates presented here, it also seems realistic that the MIS5 lacustrine thermokarst deposits with clear warm-stage indicators (Andreev et al., 2004; Ilyashuk et al., 2006; Kienast et al., 2008, 2011; Wetterich et al., 2009) and the Buchchagy IC developed both during the MIS5 *sensu lato*. If so, widespread thermokarst promoted the formation of basins and lakes by surface subsidence while the surroundings were shaped by polygon wetlands, which after the Last Interglacial developed further into the Buchchagy IC. Under this scenario it remains unknown on which ice-rich permafrost the Last Interglacial thermokarst took place.

The Last Interglacial, however, is scarcely represented in palaeoenvironmental and palaeoclimatic records from the Arctic even though northern latitudes are experiencing the strongest impact of ongoing climate warming. The uncertainty of climate variations in space and time during the Last Interglacial limits the potential of the Last Interglacial as an analogue of Holocene climate change. Hitherto, the best available palaeoclimatic record on regional scale, including the Last Interglacial, was obtained from El'gygytgyn impact crater lake sediments in Central Chukotka, Eastern Siberia (Melles et al., 2007, 2012; Chaplgin et al., 2012; Tarasov et al., 2013). Geochemical proxy data from the El'gygytgyn record give insights into climatic variability during the Last Interglacial (Cunningham et al., 2013). These records indicate the warmest climatic conditions occurred between ca. 128 and 127 kyr ago and mild conditions maintained until ca. 122 kyr ago, followed by climatic deterioration at ca. 118 kyr ago and a return of glacial conditions afterwards. The climatic instability during MIS5, which featured abrupt changes, is preserved in the geocryological inventory of Bol'shoy Lyakhovsky Island records, which mirror permafrost degradation, i.e. thermokarst (Andreev et al., 2004; Ilyashuk et al., 2006; Wetterich et al., 2009), as well as permafrost aggradation, i.e. IC formation (this study) during MIS5 *sensu lato*.

## 6. Conclusions

Palaeoenvironmental summer proxy data (pollen) of the MIS5 Buchchagy IC compare well to records from MIS3-2 Yedoma IC. Tundra-steppe vegetation is inferred for all studied periods, and the MIS5 pollen record documents drier and colder summer conditions than during the.

MIS3 interstadial and rather similar conditions to those during MIS2. MIS5 winter conditions as interpreted from the stable water isotope composition of ice wedges were also colder than during MIS3, but warmer than those during MIS2.

The unstable climatic setting of MIS5 led in non-glaciated Beringia to both intense permafrost thaw but also permafrost

formation. In permafrost records of eastern Siberia, MIS5 is mainly represented by thermokarst features like ice-wedge pseudomorphs and thermokarst lake deposits aligned to the Last Interglacial, but poorly constrained by numerical dating. The aggradation of ice-rich permafrost during MIS5 is mirrored by remnants of the Buchchagy IC firstly described in this study and dated by  $^{230}\text{Th}/\text{U}$  radioisotope disequilibrium techniques. Since convincing numerical dates of Last Interglacial thermokarst deposits are still lacking, its chronostratigraphic relation to the studied Buchchagy IC remains unknown.

## Author's contributions

SW initiated and designed the present study, and wrote the paper with contributions of the other co-authors. SW, VT and LS sampled and described the material cryolithologically. SW and LS provided sedimentological and biogeochemical data and interpretation. NR and AA provided pollen data and interpretation. VK and FM provided  $^{230}\text{Th}/\text{U}$  dating and interpretation. TO and HM provided ground ice data and interpretation. All co-authors contributed to the final discussion of obtained results and interpretations, and have approved the final version of the manuscript.

## Acknowledgements

The study was conducted under the auspices of the joint Russian-German projects *Polygons in tundra wetlands: State and dynamics under climate variability in polar regions* (POLYGON, RFBR grant № 11-04-91332-NNIO-a, DFG grant № HE 3622-16-1), *Carbon in Permafrost* (CarboPerm, BMBF grant № 03G0836B) and the *Arctic Ecological Network* (Arc-EcoNet, BMBF grant № 01DJ14003). Additional funding was provided by the Russian Federation Government to VT (grant № 2013-220-04-157) and NR (project of the Altai State University grant № 2013-220-04-129). The work of NR was furthermore supported by the Russian Science Foundation (RSF grant № 14-50-00036). The work of NR and AA in this study was performed according to the Russian Government Program of Competitive Growth of the Kazan Federal University. The work of VK and FM was supported by the RFBR (grant № 13-05-00854) and a project of the St. Petersburg State University (grant № 18.37.141.2014). The study contributes to the *Eurasian Arctic Ice 4k* project of TO (DFG grant № OP 217/2-1). We thank our colleagues who helped during fieldwork in 2007, especially Dmitry Dobrynin from Moscow State University. We are grateful to Dmitry Mel'nicenko and colleagues from the Hydrobase Tiksi, and Waldemar Schneider from AWI Potsdam who greatly supported the logistics of this expedition, and also to the team of Fedor Selyakhov from the Lena Delta Reserve who hosted our field camp at the Zimov'e River mouth in July 2007. The analytical work in the AWI laboratories was expertly conducted by Ute Bastian and Lutz Schönicke. The paper greatly benefited by helpful comments and corrections from Candace O'Connor (University of Alaska Fairbanks) and two anonymous reviewers.

## References

- Andreev, A.A., Grosse, G., Schirrmacher, L., Kuzmina, S.A., Novenko, E.Yu., Bobrov, A.A., Tarasov, P.E., Kuznetsova, T.V., Krubetschek, M., Meyer, H., Kunitsky, V.V., 2004. Late Saalian and Eemian palaeoenvironmental history of the Bol'shoy Lyakhovsky Island (Laptev Sea region, Arctic Siberia). *Boreas* 33, 319–348.
- Andreev, A., Grosse, G., Schirrmacher, L., Kuznetsova, T.V., Kuzmina, S.A., Bobrov, A.A., Tarasov, P.E., Novenko, E.Y., Meyer, H., Derevyagin, A.Y., Kienast, F., Bryantseva, A., Kunitsky, V.V., 2009. Weichselian and Holocene palaeoenvironmental history of the Bolshoy Lyakhovsky Island, New Siberian Archipelago, Arctic Siberia. *Boreas* 38, 72–110.
- Andreev, A., Schirrmacher, L., Tarasov, P.E., Ganopolski, A., Brovkin, V., Siegert, C., Wetterich, S., Hubberten, H.-W., 2011. Vegetation and climate history in the Laptev Sea region (Arctic Siberia) during late Quaternary inferred from pollen

- records. *Quat. Sci. Rev.* 30, 2182–2199.
- Arkhangelov, A.A., Mikhalev, D.V., Nikolaev, V.I., 1996. Rekonstruktsiya uslovii formirovaniya mnogoletnei merzloty i paleoklimatov Severnoi Evrazii (Reconstruction of formation conditions of permafrost and paleoclimate of northern Eurasia). In: Velichko, A.A., et al. (Eds.), *Razvitiye oblasti mnogoletnei merzloty i periglyatsial'noi zony Severnoi Evrazii i usloviya raseleniya drevnego cheloveka* (History of Permafrost Regions and Periglacial Zones of Northern Eurasia and Conditions of Ancient Man Distribution), Russian Academy of Science. Institute of Geography, Moscow, pp. 102–109 (in Russian).
- Barkova, M.B., 1982. Palynologicheskie dannye dlya stratigrafi srednego Pleistotsena poberezhya morya Laptevykh i Vostochno-Sibirskego (Palynological data for the Middle Pleistocene stratigraphy of coastal zones of Laptev and East-Siberian seas). In: Shulgina, N.I. (Ed.), *Stratigrafiya i paleogeografiya pozdnego kainozoya Arktiki* (Late Cainozoic Stratigraphy and Paleogeography of the Arctic), PGO Sevmorgeologiya. Ministry of Geology, Leningrad, pp. 90–96 (in Russian).
- Beug, H.-J., 2004. Leitfaden der Pollenbestimmung für Mitteleuropa und angrenzende Gebiete. Verlag Friedrich Pfeil, München.
- Blinov, A., Alfimov, V., Beer, J., Gilichinsky, D., Schirrmeyer, L., Kholodov, A., Nikolsky, P., Opel, T., Tikhomirov, D., Wetterich, S., 2009.  $^{36}\text{Cl}/\text{Cl}$  ratio in ground ice of East Siberia and its application for chronometry. *Geochem. Geophys. Geosyst.* 10, Q0AA03.
- Blott, S.J., Pye, K., 2001. GRADISTAT: a grain size distribution and statistics package for the analysis of unconsolidated sediments. *Earth Surf. Process. Landf.* 26, 1237–1248.
- Boike, J., Bol'shiyanov, D.Yu., Schirrmeyer, L., Wetterich, S. (Eds.), 2008. The Expedition LENA – NEW SIBERIAN ISLANDS 2007 during the International Polar Year (IPY) 2007/2008. *Reports on Polar and Marine Research* 584, p. 265.
- Börner, A., Hrynowiecka, A., Kuznetsov, V., Stachowicz-Rybka, R., Maksimov, F., Grigoriev, V., Niska, M., Moskal-del Hoyo, M., 2015. Palaeoecological investigations and  $^{230}\text{Th}/\text{U}$  dating of Eemian interglacial peat sequence of Banzin (Mecklenburg-Western Pomerania, NE-Germany). *Quat. Int.* 386, 122–136.
- Chapligin, B., Meyer, H., Swann, G.E.A., Meyer-Jacob, C., Hubberten, H.-W., 2012. A 250 ka oxygen isotope record from diatoms at Lake El'gygytgyn, far east Russian Arctic. *Clim. Past* 8, 1621–1636.
- Cunningham, L., Vogel, H., Nowaczyk, N., Wennrich, V., Juschus, O., Persson, P., Rosén, P., 2013. Climatic variability during the last interglacial inferred from geochemical proxies in the Lake El'gygytgyn sediment record. *Palaeogeogr. Palaeoclimatol. Palaeoecol.* 386, 408–414.
- Dansgaard, W., 1964. Stable isotopes in precipitation. *Tellus* 16 (4), 436–468.
- De Klerk, P., Teltewskoi, A., Theuerkauf, M., Joosten, H., 2014. Vegetation patterns, pollen deposition and distribution of non-pollen palynomorphs in an ice-wedge polygon near Kytalyk (NE Siberia), with some remarks on Arctic pollen morphology. *Polar Biol.* 37, 1393–1412.
- Elias, S.A., Brigham-Grette, J., 2013. Late Pleistocene Glacial Events in Beringia. In: Elias, S.A. (Ed.), *Encyclopedia of Quaternary Science*, second ed. Elsevier, Amsterdam, pp. 191–201.
- Ewing, S.A., Paces, J.B., O'Donnell, J.A., Jorgenson, M.T., Kanevskiy, M.Z., Aiken, G.R., Shur, Y., Harden, J.W., Striegl, R., 2015. Uranium isotopes and dissolved organic carbon in loess permafrost: modeling the age of ancient ice. *Geochim. Cosmochim. Acta* 152, 143–165.
- Fægri, K., Iversen, J., 1989. *Textbook of Pollen Analysis*, fourth ed. John Wiley & Sons, Chichester.
- Froese, D.G., Westgate, J.A., Sanborn, P.T., Reyes, A.V., Pearce, N.J.G., 2009. The Klondike goldfields and Pleistocene environments of Beringia. *GSA Today* 19 (8), 4–10.
- Geyh, M.A., 2001. Reflections on the  $^{230}\text{Th}/\text{U}$  dating of dirty material. *Geochronometria* 20, 9–14.
- Geyh, M.A., Müller, H., 2005. Numerical  $^{230}\text{Th}/\text{U}$  dating and palynological review of the Holsteinian/Hoxian Interglacial. *Quat. Sci. Rev.* 24, 1861–1872.
- Gilichinsky, D.A., Nolte, E., Basilyan, A.E., Beer, J., Blinov, A., Lazarev, V., Kholodov, A., Meyer, H., Nikolsky, P.A., Schirrmeyer, L., Tumskoy, V., 2007. Dating of syngenetic ice wedges in permafrost with  $^{36}\text{Cl}$  and  $^{10}\text{Be}$ . *Quat. Sci. Rev.* 26, 1547–1556.
- Goslar, T., Czernik, J., Goslar, E., 2004. Low-energy  $^{14}\text{C}$  AMS in Poznan radiocarbon laboratory, Poland. *Nucl. Instrum. Methods Phys. Res. B* 223–224, 5–11.
- Grimm, E.C., 2004. *TGView 2.0.2* (Software). Illinois State Museum, Springfield, Illinois.
- Grosse, G., Robinson, J.E., Bryant, R., Taylor, M.D., Harper, W., DeMasi, A., Kyker-Snowman, E., Veremeeva, A., Schirrmeyer, L., Harden, J., 2013. Distribution of Late Pleistocene ice-rich Syngenetic Permafrost of the Yedoma Suite in East and Central Siberia, Russia. U.S.G.S. Open File Report 1078, p. 37.
- Günther, F., Overduin, P.P., Sandakov, A.V., Grosse, G., Grigoriev, M.N., 2013. Short- and long-term thermo-erosion of ice-rich permafrost coasts in the Laptev Sea region. *Biogeosciences* 10, 4297–4318.
- Ilyashuk, B.P., Andreev, A.A., Bobrov, A.A., Tumskoy, V.E., Ilyashuk, E.A., 2006. Interglacial history of a palaeo-lake and regional environment: a multi-proxy study of a permafrost deposit from Bol'shoy Lyakhovsky Island, Arctic Siberia. *J. Paleolimnol.* 35, 855–872.
- Ivanov, O.A., 1972. Stratigrafiya i korrelyatsiya neogenovykh i chetvertichnykh otlozenii subarkticheskikh ravnin Vostochnoi Yakutii (Stratigraphy and correlation of Neogene and Quaternary deposits of subarctic plains in Eastern Yakutia). In: Problemy izucheniya chetvertichnogo perioda (Problems of Quaternary Studies), Nauka, Moscow, pp. 202–211 (in Russian).
- Jankowska, V., 1991. Unbekannte Objekte in Pollenpräparaten – Tardigrada. In: Kovar-Eder, J. (Ed.), *Palaeovegetational Development in Europe and Regions Relevant to Its Palaeofloristic Evolution. Proceedings of the Pan-European Palaeobotany Conference*, Vienna, 13–19 September 1991. Museum of Natural History, Vienna, pp. 19–23.
- Kanevskiy, M., Shur, Y., Fortier, D., Jorgenson, M.T., Stephan, E., 2011. Cryostratigraphy of late Pleistocene syngenetic permafrost (yedoma) in northern Alaska, Itkillik River exposure. *Quat. Res.* 75, 584–596.
- Kaufman, A., Broecker, W.S., 1965. Comparison of  $\text{Th}^{230}$  and  $\text{C}^{14}$  ages for carbonates materials from Lakes Lahontan and Bonneville. *J. Geophys. Res.* 70, 4030–4042.
- Kienast, F., Tarasov, P., Schirrmeyer, L., Grosse, G., Andreev, A.A., 2008. Continental climate in the East Siberian Arctic during the last interglacial: implications from palaeobotanical records. *Glob. Planet. Change* 60, 535–562.
- Kienast, F., Wetterich, S., Kuzmina, S., Schirrmeyer, L., Andreev, A.A., Tarasov, P., Nazarova, L., Kossler, A., Frolova, L., Kunitsky, V.V., 2011. Paleontological records indicate the occurrence of open woodlands in a dry inland climate at the present-day Arctic coast in western Beringia during the Last Interglacial. *Quat. Sci. Rev.* 30, 2124–2159.
- Konishchev, V.N., Kolesnikov, S.F., 1981. Osobennosti stroeniya i sostava pozdnego kainozoiskikh otlozenii v obnazhenii Oyogorskii Yar (Peculiarities of structure and composition of late Cenozoic deposits in the section of Oyogorsk Yar). *Problemy kriolitol.* – Problems Cryolithol. IX, 107–117 (in Russian).
- Krbetschek, M., Gonser, G., Schwamborn, G., 2000. Luminescence dating results of sediment sequences of the Lena Delta. *Polarforschung* 70, 83–88.
- Kunitsky, V.V., 1998. Ledovy kompleks i krioplannatsionnye terassy na ostrove Bol'shoy Lyakhovsky (Ice Complex and cryoplanning terraces on Bol'shoy Lyakhovsky Island). In: Kamensky, R.M., Kunitsky, V.V., Olovin, B.A., Shepelev, V.V. (Eds.), *Problemy Geokriologii* (Problems of Geocryology). RAS SB Permafrost Institute, Yakutsk, pp. 60–72 (in Russian).
- Kuprianova, L.A., Alyoshina, L.A., 1972. *Pyl'za i spory rastenii flory Evropeiskoi chasti SSSR* (Pollen and spores of the flora of the European part of the USSR). Nauka, Leningrad (in Russian).
- Kuznetsov, V.Yu., Maksimov, F.E., 2012. Metody chetvertichnoi geokronometrii v paleogeografi i morskoi geologii (Methods of Quaternary geochronometry in paleogeography and marine geology). Nauka, St. Petersburg (in Russian).
- Maksimov, F.E., Kuznetsov, V.Yu., 2010. Novaya versiya  $^{230}\text{Th}/\text{U}$  datirovaniya verkhne-i sredneneoplaestotsenovyykh pogrebennykh organogenykh otlozenii (New version of  $^{230}\text{Th}/\text{U}$  dating of the Upper and Middle Pleistocene buried organogenic sediments). *Vestnik SPBGU – Bull. St. Petersburg State Univ. Ser. 7* (4), 103–114 (in Russian).
- Maksimov, F.E., Kuznetsov, V.Yu., Zaretskaya, N.E., Subetto, D.A., Shebotinov, V.V., Zherebtsov, I.E., 2011. The first case study of  $^{230}\text{Th}/\text{U}$  and  $^{14}\text{C}$  dating of Mid-valdai organic deposits. *Dokl. Earth Sci.* 438, 598–602.
- Melles, M., Brigham-Grette, J., Glushkova, O.Y., Minyuk, P.S., Nowaczyk, N.R., Hubberten, H., 2007. Sedimentary geochemistry of core PG1351 from Lake El'gygytgyn – a sensitive record of climate variability in the East Siberian Arctic during the past three glacial-interglacial cycles. *J. Paleolimnol.* 37, 89–104.
- Melles, M., Brigham-Grette, J., Minyuk, P.S., Nowaczyk, N.R., Wennrich, V., DeConto, R.M., Anderson, P.M., Andreev, A.A., Coletti, A., Cook, T.L., Haltia-Hovi, E., Kukkonen, M., Lozhkin, A.V., Rosén, P., Tarasov, P., Vogel, H., Wagner, B., 2012. 2.8 million Years of Arctic Climate Change from Lake El'gygytgyn, NE Russia. *Science* 337, 315–320.
- Meyer, H., Schönicke, L., Wand, U., Hubberten, H.-W., Friedrichsen, H., 2000. Isotope studies of hydrogen and oxygen in ground ice – experiences with the equilibration technique. *Isotopes Environ. Health Stud.* 36, 133–149.
- Meyer, H., Dereviagin, A., Siegert, C., Schirrmeyer, L., Hubberten, H.-W., 2002. Paleoclimate reconstruction on Big Lyakhovsky Island, North Siberia – hydrogen and oxygen isotopes in ice wedges. *Permafrost. Periglac. Process.* 13, 91–105.
- Meyer, H., Schirrmeyer, L., Yoshikawa, K., Opel, T., Wetterich, S., Hubberten, H.-W., Brown, J., 2010. Permafrost evidence for severe winter cooling during the Younger Dryas in northern Alaska. *Geophys. Res. Lett.* 37, L03501.
- Meyer, H., Opel, T., Laepple, T., Dereviagin, A., Yu, Hoffmann, K., Werner, M., 2015. Long-term winter warming trend in the Siberian Arctic during the mid- to late Holocene. *Nat. Geosci.* 8, 122–125.
- Möller, P., Alexanderson, H., Funder, S., Hjort, C., 2015. The Taimyr Peninsula and the Severnaya Zemlya archipelago, Arctic Russia: a synthesis of glacial history and palaeo-environmental change during the Last Glacial cycle (MIS 5e–2). *Quat. Sci. Rev.* 107, 149–181.
- Nikolsky, P.A., Basilyan, A.E., Simakova, A.N., 1999. *Novye dannye po stratigrafi verkhnekainozoiskikh otlozenii v raione mysya Syatoi Nos* (New data on stratigraphy of Upper Cenozoic deposits in the area of Cape Syatoi Nos). In: Gribchenko, Yu.N., Nikolaeva, V.I. (Eds.), *Landschaftno-klimaticheskie izmeneniya, zhivotnyi mir i chelovek v poslednem Üleistotsene i Golotsene* (Landscape and Climate Variations, Fauna and Mankind in the Late Pleistocene and Holocene). RAS Institute of Geography, Moscow, pp. 51–60 (in Russian).
- Nikolsky, P.A., Basilyan, A.E., 2004. *Mys Syatoi Nos – Oporny razrez chetvertichnykh otlozenii severa Yana-Indigirskoi nizmennosti* (Mys Syatoi Nos – A Quaternary key section of the northern Yana-Indigirka lowland). In: Nikolsky, P.A., Pitul'ko, V.V. (Eds.), *Estestvenaya istoriya rossiskoi vostochnoi Arkтики v pleistotsene i golotsene* (Natural History of the Russian Eastern Arctic during the Pleistocene and Holocene). GEOS, Moscow, pp. 5–13 (in Russian).
- Opel, T., Dereviagin, A., Meyer, H., Schirrmeyer, L., Wetterich, S., 2011. Paleoclimatic information from stable water isotopes of Holocene ice wedges at the Dmitrii Laptev Strait (Northeast Siberia). *Permafrost. Periglac. Process.* 22, 84–100.
- Pizhankova, E.I., Dobrynina, M.S., 2010. *Dinamika poberezhyia Lyakhovskykh ostrovov – resul'taty deshifrovaniya aerokosmicheskikh snimkov* (The

- dynamics of the Lyakhovsky coastline – results of aerospace image interpretation). *Kriosf. Zemli – Earth's Cryosphere* 14, 66–79 (in Russian).
- Romanovskii, N.N., 1958. Novye dannye o stroye chetvertichnykh otlozhenii ostrova Bol'shoy Lyakhovsky, Novosibirskie Ostovava (New data about the structure of Quaternary deposits of Bol'shoy Lyakhovsky Island, New Siberian Islands). *Nauchnye Doklady Vysshei Shkoly Seriya Geologo-Geograficheskaya – Sci. Trans. Higher Educ. Geol. Geogr.* 2, 243–248 (in Russian).
- Schirrmeister, L., Oezan, D., Geyh, M.A., 2002.  $^{230}\text{Th}/\text{U}$  dating of frozen peat, Bol'shoy Lyakhovsky Island (North Siberia). *Quat. Res.* 57, 253–258.
- Schirrmeister, L., Grosse, G., Kunitsky, V., Fuchs, M.C., Krabetschek, M., Andreev, A., Herzschuh, U., Babyi, O., Siegert, C., Meyer, H., Derevyagin, A., Wetterich, S., 2010. The mystery of Bunge Land (New Siberian Archipelago) – implications for its formation based on composite palaeo-environmental records, geomorphology, and remote sensing. *Quat. Sci. Rev.* 29, 3598–3614.
- Schirrmeister, L., Kunitsky, V., Grosse, G., Wetterich, S., Meyer, H., Schwamborn, G., Babyi, O., Derevyagin, A., Siegert, C., 2011a. Sedimentary characteristics and origin of the Late Pleistocene Ice Complex on north-east Siberian Arctic coastal lowlands and islands – a review. *Quat. Int.* 241, 3–25.
- Schirrmeister, L., Grosse, G., Wetterich, S., Overduin, P., Strauss, J., Schuur, E.A.G., Hubberten, H.-W., 2011b. Fossil organic matter characteristics in permafrost deposits of the Northeast Siberian Arctic. *J. Geophys. Res. Biogeosci.* 116, G00M02.
- Schirrmeister, L., Grosse, G., Schnelle, M., Fuchs, M., Ulrich, M., Kunitsky, V., Grigoriev, M., Andreev, A., Kienast, F., Meyer, H., Babyi, O., Klimova, I., Bobrov, A., Wetterich, S., Schwamborn, G., 2011c. Late Quaternary paleoenvironmental records from the western Lena Delta, Arctic Siberia. *Palaeogeogr. Palaeoclimatol. Palaeoecol.* 299, 175–196.
- Schirrmeister, L., Froese, D., Tumskoy, V., Grosse, G., Wetterich, S., 2013. Yedoma: Late Pleistocene ice-rich syngenetic permafrost of Beringia. In: Elias, S.A. (Ed.), *The Encyclopedia of Quaternary Science*, second ed., vol. 3. Elsevier, Amsterdam, pp. 542–552.
- Schneider von Deimling, T., Grosse, G., Strauss, J., Schirrmeister, L., Morgenstern, A., Schaphoff, S., Meinshausen, M., Boike, J., 2014. Observation-based modelling of permafrost carbon fluxes with accounting for deep carbon deposits and thermokarst activity. *Biogeosci. Discuss.* 11, 16599–16643.
- Solov'ev, P.A., 1959. Kriolitozona severnoi chasti Lena-Amginskogo mezhdurech'ya (The cryolithozone of the northern part of the Lena-Amga interfluve). Academy of Science of the USSR, Moscow, p. 144 (in Russian).
- Stockmarr, J., 1971. Tablets with spores used in absolute pollen analysis. *Pollen Spores* 13, 615–621.
- Strauss, J., Schirrmeister, L., Wetterich, S., Borchers, A., Davydov, S.P., 2012. Grain-size properties and organic-carbon stock of Yedoma Ice Complex permafrost from the Kolyma lowland, Northeastern Siberia. *Glob. Biochem. Cycles* 26, GB3003.
- Strauss, J., Schirrmeister, L., Grosse, G., Wetterich, S., Ulrich, M., Hubberten, H.-W., 2013. The deep permafrost carbon pool of the Yedoma region in Siberian and Alaska. *Geophys. Res. Lett.* 40 (23), 6165–6617.
- Strauss, J., Schirrmeister, L., Mangelsdorf, K., Eichhorn, L., Wetterich, S., Herzschuh, U., 2014. Organic matter quality of deep permafrost carbon – a study from Arctic Siberia. *Biogeosci. Discuss.* 11, 15945–15989.
- Streletskaya, I.D., Gusev, E.A., Vasiliev, A.A., Oblogov, G.E., Molodkov, A.N., 2013. Pleistocene-Holocene palaeoenvironmental records from permafrost sequences at the Kara Sea coast (NW Siberia, Russia). *Geogr. Environ. Sustain.* 3 (6), 60–76.
- Tarasov, P.E., Andreev, A.A., Anderson, P.M., Lozhkin, A.V., Leipe, C., Haltia, E., Nowaczyk, N.R., Wennrich, V., Brigham-Grette, J., Melles, M., 2013. A pollen-based biome reconstruction over the last 3.562 million years in the Far East Russian Arctic – new insights into climate–vegetation relationships at the regional scale. *Clim. Past* 9, 2759–2775.
- Tikhomirov, D.A., Blinov, A.V., 2009. Cosmogenic  $^{36}\text{Cl}$  as a tool for dating permafrost ice. *Bull. Russ. Acad. Sci. Phys.* 73, 384–386.
- Tolmachev, A.I. (Ed.), 1971. Arkticheskaya Flora SSSR (The Arctic Flora of the USSR). Issue VI, Caryophyllaceae-Ranunculaceae. Nauka, Leningrad (in Russian).
- Tolmachev, A.I. (Ed.), 1975. Arkticheskaya Flora SSSR (The Arctic Flora of the USSR). Issue VII, Papaveraceae-Cruciferae. Nauka, Leningrad (in Russian).
- Tumskoy, V.E., 2009. Climatic cyclicity in a frozen deposits structure of the Eastern Arctic. In: Abstracts and Program of the Third Conference on Arctic Palaeoclimate and its Extremes (APEX), 82–83, March 31–April 3, 2009. University of Copenhagen.
- Tumskoy, V.E., 2012. Osobennosti kriolitogeneza otlozhenii severnoi Yakutii v sredнем Neopleistotsene -Golotsene (Peculiarities of cryolithogenesis in northern Yakutia from the Middle Neopleistocene to the Holocene). *Kriosf. Zemli – Earth's Cryosphere* 16, 12–21 (in Russian).
- Tumskoy, V.E., Basilyan, A.E., 2006. Key section of Quaternary deposits on Bol'shoy Lyakhovsky Island. In: Abstracts of Correlation of Pleistocene Events in the Russian North (COPERN), 106–107, December 4–6, 2006, St. Petersburg (in Russian).
- Tumskoy, V.E., Basilyan, A.E., 2009. Quaternary stratigraphy of the Dmitry Laptev Strait coasts (Northern Yakutia). In: Kontorovich, A.E., Volkova, V.S., Khazina, I.V., Khazin, L.B. (Eds.), Proceedings of the 6th All-Russian Quaternary Conference. RAS SB Publishers, Novosibirsk, pp. 592–593 (in Russian).
- Tumskoy, V.E., Dobrynnin, D., 2008. Stratigraphical and geomorphological studies along the south coast of Bol'shoy Lyakhovsky Island and along the Oyogos Ya coast. *Rep. Polar Mar. Res.* 584, 41–50.
- Tumskoy, V.E., Maksimov, F.E., Kuznetsov, V.Yu., 2015. Geokhromonetricheskie dannye o vozraste pozdnopleistotsenovyxh otlozhenii ostrova Bol'shoy Lyakhovsky, Novosibirskie ostrova (Geochronometric data of late Pleistocene deposits of Bol'shoy Lyakhovsky Island, New Siberian Islands). *Kriosfera Zemli (Earth's Cryosphere)* (submitted for publication).
- van Everdingen, R.O. (Ed.), 1998. Multi-language Glossary of Permafrost and Related Ground Ice Terms. Arctic Institute of North America. University of Calgary.
- van Geel, B., 2001. Non-pollen palynomorphs. In: Smol, J.P., Birks, H.J.B., Last, W.M. (Eds.), *Terrestrial Algal and Siliceous Indicators, Tracking Environmental Changes Using Lake Sediments*, vol. 3. Kluwer Academic Press, Dordrecht, pp. 99–119.
- Vasil'chuk, Y.K., Vasil'chuk, A.C., 2014. Strategy of valid  $^{14}\text{C}$  dates choice in syngenetic permafrost. *Cryosphere Discuss.* 8, 5589–5621.
- Wetterich, S., Kuzmina, S., Andreev, A.A., Kienast, F., Meyer, H., Schirrmeister, L., Kuznetsova, T., Sierralta, M., 2008. Palaeoenvironmental dynamics inferred from late Quaternary permafrost deposits on Kurungnakh Island, Lena Delta, Northeast Siberia, Russia. *Quat. Sci. Rev.* 27, 1523–1540.
- Wetterich, S., Schirrmeister, L., Andreev, A.A., Pudenz, M., Plessen, B., Meyer, H., Kunitsky, V.V., 2009. Eemian and Late Glacial/Holocene palaeoenvironmental records from permafrost sequences at the Dmitry Laptev Strait (NE Siberia, Russia). *Paleogeogr. Paleoclimatol. Paleoecol.* 279, 73–95.
- Wetterich, S., Rudaya, N., Tumskoy, V., Andreev, A.A., Opel, T., Schirrmeister, L., Meyer, H., 2011. Last Glacial Maximum records in permafrost of the East Siberian Arctic. *Quat. Sci. Rev.* 30, 3139–3151.
- Wetterich, S., Tumskoy, V., Rudaya, N., Andreev, A.A., Opel, T., Meyer, H., Schirrmeister, L., 2014. Ice Complex formation in arctic East Siberia during the MIS3 Interstadial. *Quat. Sci. Rev.* 84, 39–55.
- Zaitsev, V.N., Solov'ev, V.A., Pletnev, V.E., 1989. Yano-Kolymskoi region (Yana-Kolyma region). In: *Geokriologiya, S.S.R. (Ed.), Vostochnaya Sibir' i Dal'nyi Vostok (Geocryology of the USSR. East Siberia and Far East)*. Nedra, Moscow, pp. 240–279.
- Zimov, S.A., Schuur, E.A.G., Chapin, F.S., 2006. Permafrost and the global carbon budget. *Science* 312, 1612–1613.